An Analysis of the Symmetry of Large Cutting Tools within the South African Acheulean

Raymond Alexander Couzens

A dissertation submitted to the Faculty of Science, University of the Witwatersrand, Johannesburg, in fulfilment of the requirements for the degree of Master of Science

Johannesburg 2012

DECLARATION

I declare that this thesis is my own, unaided work. It is being submitted for the Degree of Master of Science in the University of the Witwatersrand, Johannesburg. It has not been submitted before for any degree or examination in any other University.

_____

(Signature of candidate)

Raymond Couzens

_____day of _____20_____

ABSTRACT

The use of three dimensional modelling techniques with reference to the study of archaeological material is one that is gaining popularity in hominid studies and is already being extensively used globally. This research delves deep into the Acheulean period and takes a refreshed look at the symmetry of handaxes from two sites, namely Rietputs 15 (1.4 ma) which is an early Acheulean site, and the Cave of Hearths, which is estimated to *ca* 450/500 000 years old and forms the later Acheulean aspect of this sample. This research focuses on creating effective methods for studying symmetry in relation to various variables specific to each site, and it aims to gather data using 3D methods that more traditional 2D techniques struggle to capture. Ultimately this data provided me with a quantified measure of symmetry for handaxes from the two sites. For the Cave of Hearths, statistical evaluation of the measures of left versus right volumes showed strong, statistically significant correlations ($r = 0.870$, $p < 0.05$), as did measures of left versus right surface areas ($r = 0.960$, $p < 0.05$). Rietputs provided comparable results of: $r = 0.859$, $p < 0.05$ for volume, and $r = 0.954$, $p < 0.05$ for area, thus suggesting that good symmetry exists. By using sectoral analysis, this study shows that the tip is the most variable sector of the tools for both sites. This result supports the assumption that handaxes were designed for varied functions (e.g., cutting, skinning, digging roots, or working wood) but ones which required a strong distal end. The medial and proximal sectors are both relatively less variable, and their properties may have been more constrained by the convergent shape of the tool. Values for the later Acheulean sample show only slightly less variability than for the early Acheulean, but this is nevertheless an interesting trend which relates to hominid and cultural evolution over ca 1 million years of time.

ACKNOWLEDGEMENT

I would like to firstly thank the Palaeontological Scientific Trust (PAST) and the National Research Foundation (NRF) for the funding that made a majority of this research possible. I would also like to give thanks to the Institute for Human Evolution (IHE) for purchasing the scanning hardware and software necessary for this project. I thank all the individuals who helped train me in using the associated software and made me feel welcome within the IHE department. I would especially like to thank my co-supervisor Dr Kristian Carlson for providing limitless help within the 3D and statistical world. I would further like to thank Dr Alexandra Sumner for supporting me during my research and being someone with whom I could easily discuss my opinion. I would like to extend a thank you to Professor Terrance McCarthy for his expert opinion in helping me identify the raw materials of my specimens. Lastly I would like to give enormous thanks to my principle supervisor Professor Kathleen Kuman for guiding me through the last two years. It has been quite a journey and I would not have completed this thesis without her input.

DEDICATION

This thesis is dedicated to my mother and father for getting me interested in Archaeology before I could write out the alphabet, let alone complete a Masters thesis.

TABLE OF CONTENTS

LIST OF FIGURES

LIST OF TABLES

CHAPTER 1: INTRODUCTION

1.1 Introduction

The Acheulean period is one of extreme length and absolute importance for researchers attempting to understand the thought processes that helped in the evolutionary progression from early tool producers such as *Homo ergaster* to *H. sapiens*. Within this time period a purely unique tool form known as the handaxe was being produced. Due to the fact that handaxes are the most purposefully shaped tool in the Earlier Stone Age and exhibit significant variations of form, they have caused researchers to invest a much more considerable amount of effort into their research than other tool types of the Early Stone Age.

In recent literature, symmetry and standardisation of stone tools are thought to have improved with time. This study takes an in-depth look at this phenomenal stone type in the 3D realm and seeks to apply a methodology that builds upon older more traditional techniques in order to study symmetry in a more comprehensive three-dimensional way.

The Acheulean techno-complex follows the Oldowan tradition for East Africa in time, first appearing at around 1.76 ma in the Nachukui Formation, West Turkana, Kenya (Lepre *et al.* 2011). A second early date of 1.7 ma for the Acheulean exists for the East African site Konso Gardula in Ethiopia (Beyene *et al.* 2007). Other sites such as Olduvai Gorge exhibit dates for the Acheulean that range between 1.6 and 1.4 ma respectively (Hay 1976; Isaac 1997).

For southern Africa, the number of sealed Acheulean sites that exist or are able to be reliably dated is minimal. Thus we rely mainly on relative dating through faunal comparisons with East African assemblages (such as those mentioned above) where absolute dating is feasible because of the presence of dateable volcanic sediments (Klein 2000; Kuman 2007). More recently the cosmogenic nuclide burial method has been applied by Gibbon *et al.* (2009) to the Rietputs Formation (near Windsorton in the Vaal River basin, about 1.5km from the modern Vaal river (Figure 1), and dates for the early Acheulean in southern Africa now range between 1.69 ± 0.17 and 1.14 ±0.20 ma (Gibbon

et al. 2009; Kuman pers comm.). These dates suggest a well dispersed use of Large Cutting Tools (LCT's) in Africa by ca. 1.6 ma (Gibbon *et al.* 2009).
The handaxe sample from Rietputs 15 (n=33 excluding tipless types) makes up the early Acheulean part of my sample and is dated to ca 1.4 ma (Gibbon *et al.* 2009). It was retrieved by George Michael Leader from diamond mining operations in 2007 as part of his MSc research (Leader 2009). Some earlier work had been done on the site by C. van Riet Lowe and the Abbé Breuil at the time when Windsorton was an active diamond mining town (van Riet Lowe 1945).

The Cave of Hearths handaxes represent the later Acheulean aspect of this sample (n=31 excluding tipless specimens). The site is located in the Limpopo Province some 15km from Makopane (formerly Potgietersrus). More specifically the actual cave can be found on the southern slope of the Mwaridzi valley which is actually a smaller portion of the much larger Makapansgat Valley (McNabb *et al.* 2004) (see Figure 2). The site was discovered by van Riet Lowe in 1937 and excavations were carried out by Guy Gardner, James Kitching and Revil Mason between 1947 and 1957. Later one of the most important finds, a hominin mandible attributed by Tobias (1971) to *Homo sapiens rhodesiensis*, was discovered in Bed 3 (McNabb *et al.* 2004). The sample represented in this study comes from Beds 1-3. It is typical of the later Acheulean in a number of ways. Some researchers group the mandible with *Homo heidelbergensis* and thus a date of ca. 400-500 ka for these beds is generally accepted (McNabb *et al.* 2004). The site is one of utmost importance when considering the Stone Age in South Africa, particularly as it contains a long sequence including the Earlier, Middle and Later Stone Age (McNabb *et al.* 2004).

The comparison between these two handaxe samples thus relates to an extreme temporal scale (between 1.4 ma and ca 0.45 ma) and this remains the main reason for their selection in this research. If trends occur in symmetry or standardization, they should be easier to determine at these two extremes in time and should help us better understand the Acheulean in southern Africa.

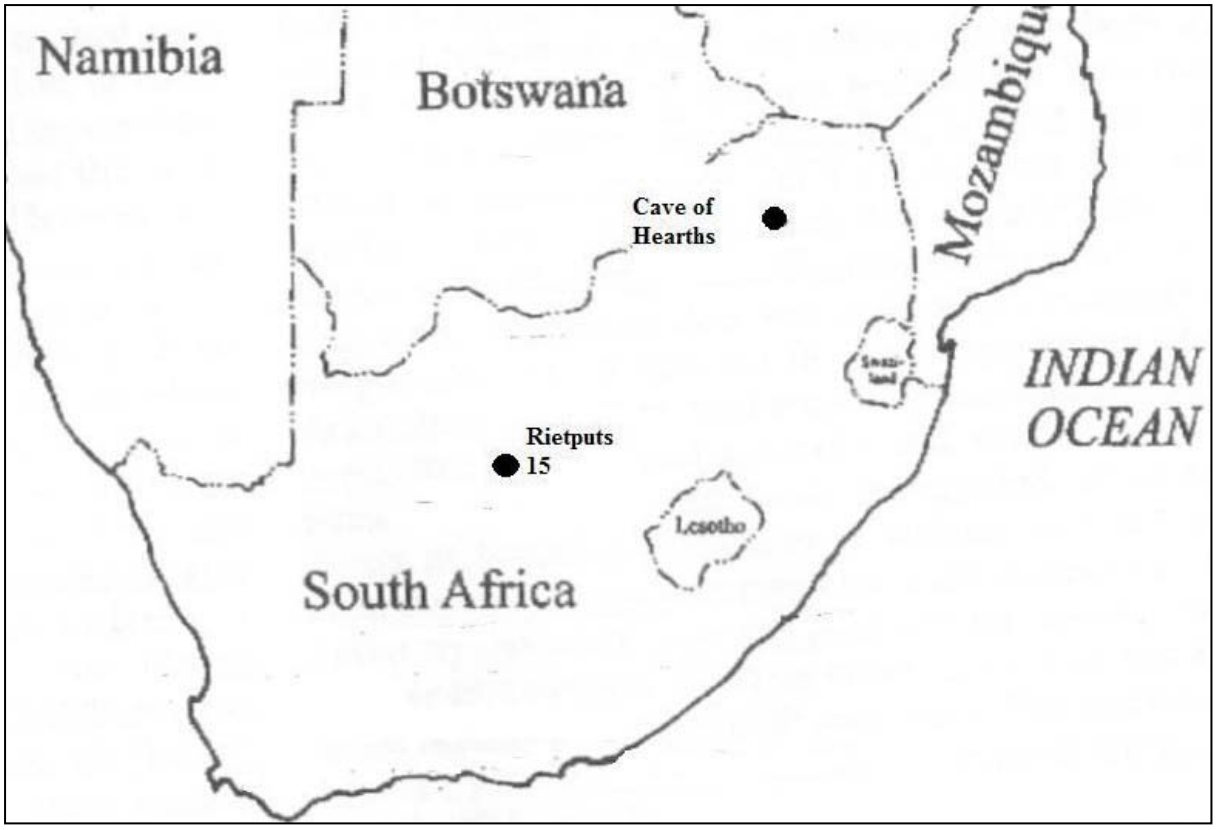

Figure 1: Map depicting locations of Rietputs 15 and the Cave of Hearths

1.2 Research Goals

Because most handaxes are considered to be commonly shaped to a tip and are bilaterally symmetrical, researchers such as McNabb *et al.* (2004) argue that some kind of cultural, symbolic or functional action must be at play in the minds of the makers.

This study aims to look at the symmetry of handaxes from the above mentioned sites mainly because of the explicit features identifiable in each sample. More specifically, many early Acheulean handaxes from Rietputs 15 are shaped to a rather crude, robust or pick-like tip, while the later Cave of Hearths handaxes seem to be better worked around their edges and also are better worked at the tip. The in-depth study of these characteristics could hold some functional or stylistic value in their interpretation and thus the study of their standardization or lack thereof could be important considering the long temporal scale that is available to this study (McNabb *et al.* 2004; Leader 2009).

The use of three-dimensional modelling techniques with reference to the study of archaeological material is a discipline that is gaining popularity in current studies, and

new research is constantly being produced as an effect of the exponential rate of improvement in modern day technology. Three-dimensional studies are important because they can produce highly accurate measures such as the more common length, width and thickness applied in archaeology, as well as provide advanced measures such as volume, surface area and centre of mass that have until quite recently been understudied. The manufacture of three-dimensional databases is also important to archaeology because they provide easily accessible data that can be shared across borders without the potential risk of any type of damage occurring to a given assemblage (Sumner & Riddle 2008).

This study stands to establish a suitable methodology for assessing symmetry that can be applied to complete handaxes through the use of a portable laser scanner. It draws on ideas often used during the traditional documentation of tools but primarily aims to build upon these in a three-dimensional way, taking into account variables such as the raw material and blank types present in the tools for each site. Put more explicitly, it aims to show standardization or lack thereof for early and later Acheulean assemblages, as well as assist in creating a new method for handaxe alignment within the three -imensional realm that is based primarily on what Grosman *et al.* (2008) calls the intrinsic morphology of the tool at hand. The method put forward here is self-contained by the object being studied and offers an extremely simple way of aligning handaxes for three-dimensional research to obtain values such as volume and surface area, which more classical methods struggle to quantify. The contribution of this research is to portray the nature of the Acheulean in greater detail than more traditional methodologies allow, ultimately taking us deeper into the minds of the makers of these tools.

CHAPTER 2: LITERATURE REVIEW

2.1 The Acheulean and change through time

In East Africa, the earliest Acheulean begins at 1.76 ma from the Nachukui Formation in West Turkana, Kenya (Lepre *et al.* 2011); a second and more recent early date has been established at about 1.7 ma at Konso Gardula, Ethiopia (Asfaw *et al*. 1992; Beyene *et al.* 2007). Other sites in the Rift Valley date between 1.6 and 1.4 ma, namely East Lake Turkana (Kenya) and the middle and upper subdivisions of Bed II at Olduvai Gorge (Hay 1976; Isaac 1997). The latest date for the Acheulean is yet to be firmly established, but Porat *et al.* (2010) suggest that the Middle Stone Age (MSA) replaces the Acheulean at a minimum of 464 ± 47 ka, according to recent OSR dates from Kathu Pan. For Kenya, Ethiopia and Zambia, reliable estimates show that the Acheulean is replaced by the MSA between 250 to 200 ka (Klein 2000). The Acheulean period thus spans an extensive time period before it is arguably replaced by the Middle Stone Age some 250-200 ka according to Klein (2000).

The earliest confirmed Acheulean sites in southern Africa occur in two localities, namely the Sterkfontein valley, (consisting of sites such as Sterkfontein, Swartkrans and Kromdraai A in Gauteng Province) and the alluvial deposits of the Rietputs Formation located in the lower Vaal River basin (Kuman & Gibbon, in press). Handaxes have been found at both Sterkfontein and Swartkrans, and although no handaxes or cleavers were found at Kromdraai A, the site is still regarded as Acheulean (Kuman *et al.* 1997). The artefacts at these three sites are thought to have belonged to the same industry in that they are all very similar according to Kuman & Gibbon (in press). Sterkfontein Member 5 contains a fragmentary fossil of *Homo ergaster* and is estimated to be about ± 1.5 ma (Kuman & Clarke 2000), Swartkrans Members 2 and 3 are estimated to date ca. 1.5 and 1.0 ma respectively (Kuman & Gibbon in press). Emphasis on the tips of tools from Sterkfontein and Swartkrans seems apparent as most exhibit a very sturdy and often pick-like nature which could have related to their function (Kuman and Gibbon in press).

For South Africa Gibbon *et al.* (2009) suggest that the cosmogenic nuclide burial dating of the Rietputs Formation is important because it captures very early absolute dates for the Acheulean outside of Gauteng Province, where relative faunal dating has been used at the

Cradle of Humankind sites. In this case, dates for the early Acheulean at Rietputs range between 1.69 ± 0.17 and 1.14 ± 0.20 ma for individual artefacts or clasts containing quartz. The layer is sealed by a fine alluvium lacking artefacts with a date of 1.26 ± 0.10 ma (Gibbon *et al.* 2009). The large error margin in the earliest appearance date conforms to an age of 1.6 ma. The Cradle of Humankind and Rietputs Formation results therefore suggest a rapid and well distributed spread of handaxes and their users within southern Africa and throughout Africa by *ca* 1.6 ma.

Kuman (2007), like Mason (1962), believes that between the early Acheulean (1.7 to *ca* 1 ma) and the later Acheulean (0.6 to 0.2 ma), a "middle" Acheulean phase exists that may be applicable to some South African sites based on associated fauna or on lithic typologies. Kuman (2007) points out that many researchers avoid this debate and allocate all sites younger than or equal to 1 ma into the "upper" Acheulean. However, the concept of a "middle Acheulean" is important because (and this has become apparent at Olduvai Gorge) it increases the resolution of the details related to technological change over time. This change is apparent when considering the tools excavated from Olduvai Gorge Beds II to IV (dated 1.60 to *ca* 0.8/0.6 ma) and post Bed IV (dated ca. 0.6-0.4). In these deposits, handaxes develop from thicker and less standardized forms in Bed II to more regularized shapes (and more cleavers) in Bed IV later Acheulean (Roe 1994). After Bed IV in time, artefacts exhibit characteristics that indicate increased technological control. A similar pattern occurs in the Middle Awash region of Ethiopia, where earlier Acheulean LCT's *ca* 1 ma (‘’middle Acheulean’’) in the Daka Member are followed by more refined examples from the Herto Member *ca* 0.4 ma (later Acheulean). In terms of technology, the progression through time resembles that of Olduvai Gorge beds following the early Acheulean (Schick & Clark 2003). In addition the long sequence at Olorgesailie in Kenya, dated 0.99 ma to 0.49 ma (Isaac 1977; Potts 1989), provides further examples of "middle" to "later" Acheulean assemblages in East Africa. The identification and dating of "middle Acheulean" assemblages in South Africa now also appears feasible with current research in the Vaal River basin (Kuman, pers. comm).

Large Cutting Tools such as the handaxe, cleaver and pick [Mode II artefacts, described by Clark (2001)]signal the beginning of the Acheulean and are often said to be made according to a "mental template" because they are all commonly shaped to a point (in the case of handaxes and picks) or to a broad cutting edge in the case of cleavers (Wynn 1995; Klein 2000; Kuman 2007). In most cases early Acheulean bifaces (a generic term often used for

handaxes and cleavers) are, according to Klein (2000: 110): "thicker, less extensively trimmed and less symmetric than later ones". Tools of this time very often have less than 10 removals, with deep scar patterns indicating a hard hammer technique. Trihedral, pick-like handaxes are also common in some early Acheulean assemblages (e.g., Asfaw 1992). This contrasts with later Acheulean bifaces which can be very thin, bilaterally symmetrical, sometimes intensely worked, and finished with soft hammer percussion resulting in greater regularity of form (Klein 2000; Goren-Inbar & Sharon 1999; Goren-Inbar & Sharon 2006). Crude bifaces also exist in the later Acheulean, but the general trend is toward a more refined technique.

It is uncertain as to why the symmetry of handaxes increased over time, but it has been suggested that differences in handaxe morphology could be based on functionality (Clark 2001), rather than increased cognitive ability as suggested by Klein (2000). The pick-like nature of many early handaxes (e.g., Asfaw 1992) could indicate that functions other than butchery may have been prominent in the early Acheulean, for example, digging for roots. Replicative experiments have revealed that the sharp edges of handaxes could have been useful for the cutting and/or skinning of game (Toth 1985); and experimental studies on cut-marked bone at Swartkrans by Pickering *et al.* (2008) further confirm this prognosis. With regard to variability, Clark (2001) suggests that the selection of raw materials and functionality plays the greatest role in the morphological variations among tools, although he stipulates that aspects such as environment and age or skill level of the knapper (although unidentifiable at present) should also be considered. The opportunistic availability of raw material can also lead to variability of tool attributes (Clark 2001; Klein 2000).

Work by Crompton & Gowlett (1993) using mathematically predictive techniques known as allometry has suggested that variability can be explained by size of the blank at the time of production. They explain that a bigger blank type would lead the producers to make sacrifices to other parts of the tool in order to keep the tool balanced in terms of weight thus resulting in varied shape (Crompton & Gowlett 1993; McPherron 2000).

2.2 Handaxe symmetry and its traditional study

The handaxes of the Acheulean period exhibit the most classical item of study for researchers attempting to understand hominid cognition because they are so unique in form. In

archaeology the term bilateral symmetry is used to describe an object that appears to have equal and opposite sides that mirror each other when viewed on a plane (for 3D) or viewed on an axis (for 2D). The study of this sort of phenomenon is one that has received attention from many different intellectual sectors including art and science (Gowlett 2011; Saragusti *et al.* 2005).

Traditionally ways to describe handaxes were based on what Grosman *et al.* (2008) described as a 'language'. This language consisted of two divisions: the descriptive and the metric. The former pertains to basic labelling of form, for instance the term tear drop shaped, while the latter describes tools in terms of simple measurements such as length, width and thickness. It also makes use of ratios such as the index of refinement (which put mathematically is maximum thickness divided by maximum width) used by Roe (1968), and the index of elongation (width divided by length) cited by McPherron (2000). These ratios can be simply used to define certain properties of a handaxe. The index of refinement basically indicates handaxe modification so when the ratio is larger the handaxe will be more unrefined (Grosman *et al.* 2008). The same applies for the index of elongation, which indicates how long a handaxe is based on the ratio given (McPherron 2000). The use of allometry (which is a predictive mathematical model mentioned above) has also been used by Crompton and Gowlett (1993) to give functional explanations about the shape of artefacts. Allometry basically describes how the physical attributes of a tool react to one another when one attribute of form is modified, i.e. what happens to width when length is increased.

In early studies, handaxes were generally considered to be symmetrical based upon the use of the methods described above, but it is becoming more obvious that these hypotheses are merely based on assumption and that qualitative studies, although useful in certain contexts, can only offer very little about a given assemblage in its macro scale. Various authors in the realm of lithics posit that qualitative studies do not adequately account for the variability shown amongst handaxes that span broad geographical as well as temporal contexts (Archer & Braun 2010; Grosman *et al.* 2008; Clarkson 2001; Saragusti *et al.* 1998, 2005). One such example of a study of symmetry based on loose qualitative methodology is McNabb, Binyon and Hazelwood's By-Eye test that was carried out on the Cave of Hearths handaxes (McNabb *et al.* 2004), on which this present study focuses. Their test for symmetry involved dividing a given tool up into six sectors before mentally imagining the tool folded along its long axis and then giving each sector a simple yes or no score as to whether or not it was deemed

symmetrical. This method was challenged by Underhill (2007), and while aspects of the study were useful such as the explanation of tip types and the increased rate of study for the tools, the measure of actual symmetry was a highly subjective one.

Saragusti *et al.* (1998, 2005), in contrast,provide a method to measure symmetry quantitatively, which they use to help explain variability on an inter- and intra- assemblage basis. The Continuous Symmetry Measure (CSM) proposed by Saragusti and colleagues displays "the minimal distances that the vertices of a shape have to go to attain the desired symmetry" through the use of mathematical equations or algorithms (Saragusti *et al.* 1998.819). At the same time, the method discards ambiguous descriptive terms that are used in more classical works.

With recent progress in modern technology, it is possible to develop an alternative way of deriving symmetry. The field of geometric morphometrics, which has been in existence for the last 20 years or so, can bridge the gap between the second and third dimensions of handaxe analysis using mathematical formulae to replicate aspects of shape (Grosman *et al.* 2011). A few different studies exist: the Wynn and Tierson (1990) method involves creating 22 polar co-ordinates originating from the midpoint of the long axes to the outer reaches of the object using a digitizer. Although deemed problematic their method basically aided in explaining typological variations of form (Underhill 2007).

Brande & Saragusti (1996) also produced a computer program whereby 2-D linear landmark measurements could be converted into 3-D geometric models that better describe shape. However, Saragusti *et al's.* algorithms are limited because they have been labelled as extremely mathematically complex and the software for their use is difficult to obtain (Cardillo 2010; Hardaker & Dunn 2005; (Underhill 2007). Brande & Saragusti's (1996) method of alignment was the same as Roe's alignment.

Lycett *et al.* (2006) also make use of three-dimensional morphometrics to evaluate the shape of Pleistocene cores, combining their study with a biological phylogenetic approach. By using multivariate statistical analysis, they were then able to search for larger trends pertaining to asymmetry, amongst other variables (Cardillo 2010; Lycett *et al.* 2006).

Archer & Braun (2010) draw on Lycett and his partners' work by applying a geometric

morphometric method to the handaxes from the Acheulean site of Elandsfontein. In order to show that handaxe variability could be related to a specific reduction strategy based on raw material availability or selectivity, they used a 3D digitizer and produced various models (Archer & Braun 2010).

Another example of a tool that can be used for quantitative study (although it is not a three-dimensional one) is Hardaker & Dunn's (2005) Flip Test. The test is a freely downloadable program that was designed primarily for work on handaxes. Using photographs and/or artistic sketches, they fold the tool over across its long axis. The overlapping pixel count can be calculated to show asymmetry using an index compiled by the authors (Hardaker & Dunn 2005). The test is useful because it is easy to obtain and easy to apply, but conversely, it does exhibit some problems with the alignment of tools, which is something that Grosman *et al.* (2008) explain is problematic in recent lithic studies. More recently academics have been delving deeper into the use of three-dimensional modelling techniques as a way of advancing lithic studies. Three-dimensional studies are practically limitless in what they can be used for and can be applied to many existing artefact types, including stone, bone, ceramics, textiles, and even sites can be reconstructed in this way (Sumner & Riddle 2008). Three-dimensional modelling is useful because the complete surfaces of an object can be created and viewed with simplicity rather than working with digitised co-ordinate values which are numerical and can confuse the user during the reconstruction of the object in question (as in Saragusti *et al's.* work). This section shall briefly describe a few instances whereby newer three dimensional techniques are being applied to lithic technologies. It will also discuss some of the advantages and disadvantages encapsulated therein.

Sumner & Riddle (2008) used photogrammetry to recreate an exact 3-D replica of an Acheulean handaxe, as well as reconstruct the surfaces of refitted Middle Paleolithic cores from Egypt in 3-D to examine the core reduction strategy. The methods that the writers used in their study are quite similar to the ones presented in the next chapter, although their method is more affordable because all that is needed is a laptop, a digital camera and some 3-D software. In their photogrammetric study, the authors explain that each object was photographed in such a way that an overlap of images could be produced and later merged. This step differs significantly when compared to my method in terms of time frame, as Sumner & Riddle (2008) explain that the merge process is done manually and could take up to 10 hours for an experienced researcher. Turnover rate is one instance where three-

dimensional laser scanning seems to have the upper hand for lithic studies.

Regardless of the time implications, Sumner & Riddle (2008) were more focused on the advantages of using three-dimensional modelling in archaeology and their study certainly proves this in a number of ways. They suggest that the advantages of using 3-D is tenfold because models can be accessed anywhere in the world through the internet. They also explain that entire assemblages can literally be examined with the touch of a button, and that by doing so in this way, real assemblages can be better preserved or not subjected to handling damage (Sumner & Riddle 2008). The ability to study cross sections of an original specimen is one that should be considered invaluable to modern studies.

A second important output is that the 3-D programs used to model objects are equipped with applications that allow for the direct accurate calculation of a variety of different values. Three-dimensional programs such as Avizo 6 (used for this study) make it easy for researchers and even the general public to obtain information about an object in a highly manageable way. These programs offer tools that can provide the most basic metric calculations which traditional approaches struggle to capture, such as surface area, volume and centre of mass (Grosman *et al.* 2008; Sumner & Riddle 2008).

Another recent study by Lin *et al.* (2010) used three-dimensional scanning to assess whether 3D measures were more precise for cortex areas than mechanically averaged measurements. Their study showed that three-dimensional measures were more accurate when sample sizes were larger than those of individually measured specimens furthermore, cementing the fact that three-dimensional techniques are applied better in quantitative case studies.

2.3 Three-dimensional scanning and the future

Despite the multitude of practical uses of three-dimensional scanning, there are in fact problems within the discipline that need to be overcome through experimentation with different techniques. Grosman *et al.* (2008) suggest that because uneven and/or perhaps asymmetric objects offer different metric measures according to how they are aligned, it is clear that ambiguities and ‘errors’ will exist from study to study. They go on to further explain that: “the intrinsic impossibility to find a ‘true’ or ‘unique’ positioning is a mathematical fact that cannot be circumvented” (Grosman *et al.* 2008: 3102).

Grosman and her colleagues designed a computer-formulated algorithm based on complex mathematical design to apparently create an unambiguous alignment (or alignments) for artefacts, as well as to better document new measures available to 3-D scanning. This study in the greater scheme of things produces better information on the application of three-dimensional modelling techniques to archaeology. It also shows that newer computer technologies can reduce human error significantly and rejuvenate traditional paradigms in a refreshed light (Grosman *et al.* 2008).

Although our methodologies differ significantly, the overall concept of the above mentioned study to better understand the past through the future of technology is also the underlying feature of this study. The method discussed in the next chapter is one that is extremely simple to grasp and apply to any handaxe, without having to wade through complex mathematical procedures. It is equally quite affordable and all the data can be easily transmitted upon request. It is my expectation that it will greatly add to the pool of knowledge for three-dimensional lithic studies.

CHAPTER 3: METHODOLOGY

This section will explain the methodology and equipment I used in order to gauge symmetry for the handaxes in my study. There are two phases: the scanning and the editing of scans.

As previously noted, the alignment or correct positioning of a given tool is not straightforward, especially in a three-dimensional analysis. My study seeks to provide researchers with a way of aligning handaxes that is based solely on the intrinsic dimensions of the tool being studied. Although the alignment is based on two dimensions, the measures it creates ultimately provide the most accurate three-edimensional data, such as volume and surface area values. The accuracy is greatly improved over the values obtained with more traditional measurements in 2D. This study did not use Roe's (1964) measurement method (Figure 2) for studying handaxes, which divides the tool into eight sectors. Instead I separated each tool into six sectors, each representing 16.65%, because I wanted to break away from traditional measures. In addition, McNabb *et al's.* (2004) by-eye test had already been applied to one of my sites (Cave of Hearths) for determining symmetry based on sectoring a tool into six sectors. This study seeks to quantify their results in a more accurate fashion with 3D scanning.

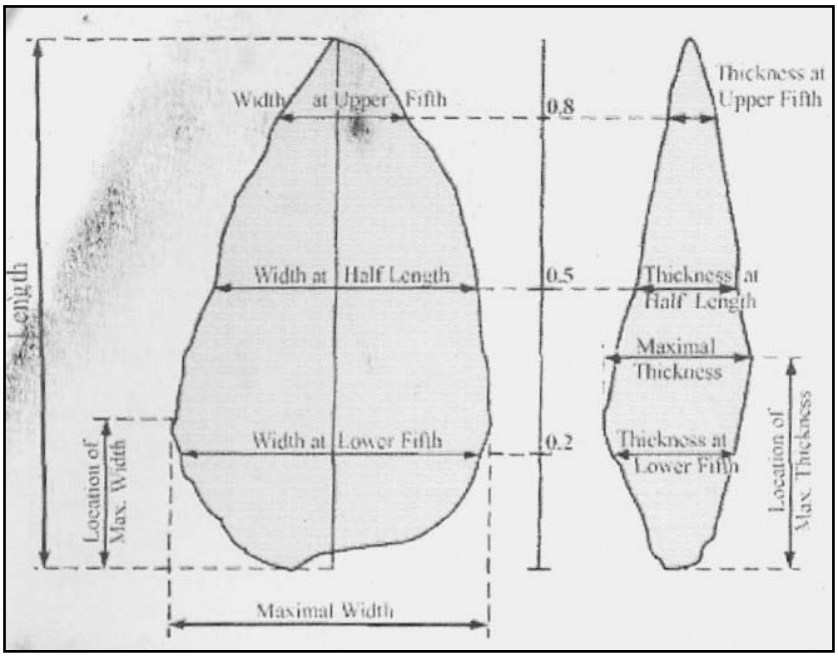

Figure 2: Conventional positioning and measurement extraction (from Roe, 1964 and after Grosman *et al.* 2008)

3.1 Scanning

The equipment employed is a portable scanner called the Real Scan USB version 5.50.12.15 COM, which is manufactured by 3D Digital Corp 2008 and was purchased by the University of the Witwatersrand at the end of December 2010.

Figure 3: Depicting Real Scan USB scanner, table and scanning stand

The scanner (shown in Figure 3) is easily assembled and a dimly lit room is more than adequate for the scanning process to take place. The scanner is fixed to an adjustable tripod and angled either facing the object straight on or at a downward angle. The scanning table was covered in black velvet to reduce light reflectivity and minimize background noise, because both of these can affect the outcome of the scan adversely. Tools were then fixed to a pottery wheel using either Prestik or black modelling clay (the base/circumference of the wheel was also covered in black cardboard). The wheel was then marked at every 45 degrees to ensure a maximum amount of overlap during the scanning process, as well as to provide the researcher with a point of reference when scanning. The scanner is then set up to face the tool (see Figure 3).

The scan process integrates several pre-scanning exercises. The most important is the Preview Window, which allows the viewer to manipulate the actual scanner specifications and fine tune the limits of the scanner before the formal scanning begins. The extent of the laser can be manipulated in the X/Y and Z dimensions. This means that the laser can be set to scan certain parameters. For example, the maximum scan area from left to right is the X

value, the Y value is determined by the angle of the scanner on the tripod (which can be adjusted if an object to be reviewed is too large), and the Z value represents the maximum distance or depth of field of the laser. The intensity of the laser beam can also be set depending on the amount of detail that is wanted. For each scan in this study, I scanned all tools at the maximum resolution of 255 points and 200 lines per tool (which results in up to 20,000 triangles of data created). One can do preview scans while manipulating the aforementioned variables, and once happy with the settings, a formal scan can be started.

The tool is rotated and scanned every 45° until it has done a complete 360° circuit, ensuring that the rotation is uniform. The scans follow in order, which creates eight scan images, but more can be done depending on the amount of detail required. The base of the tool needs to be scanned by holding the butt end straight into the laser and taking multiple scans, or by just laying it flat on the podium and turning it over a few times. The former method, however, generally produces much better scans. About 10 scans are needed to produce a full 3-D image of a handaxe.

3.1.1 Cleaning and Merging

The next step in the scan process involves the use of software that is designed to clean the images and merge each individual scan to the next one, using Slimwiz software. Each scan can be loaded into an erasing wizard whereby unwanted areas of a scan such as background noise can be manually removed simply and efficiently. This was particularly useful for cleaning up the butt end of a tool because it would often contain noise, such as my hands or the Prestik used to secure the tool to its platform. For the merging of the scans, scan files are loaded into the Slimwiz program and a reference image is selected as a starting point for each scan in the sequence to relate back to should the software experience difficulty during an alignment, normally the butt end is chosen because all scans should include some portion of that particular scan. Scans are successively merged with one another in the sequence beginning with the scan acquired subsequent to the reference image. The merging process then shows four windows (see Figure 4). The merge process works on a triangular point system whereby similar overlapping landmarks are placed on two adjacent images, each shown in a screen of its own (top left and right), and a final merge screen (bottom right) creates a best fit aspect, which the researcher can refer to when merging. The last window (bottom left panel) indicates the matching ratio between the points during merging; a lower

value means a closer fit between the scans. The software manual suggests that a value under 5 is reasonable, but for this study I aimed for a value of under 1 (i.e., 0.1 or 0.2), although values such as 1.1 or 1.2 were also accepted. The programme allows you to check your merges and to make changes before saving your full 3D image in a multitude of formats (in this case: .Stl format). Figure 5 provides an example of a full merge with an incompatible surface that will need to be changed before it is saved).

The merging process can be done manually or automatically, although manual alignment was preferable in this study. The scanning of tools can be done at a rate of about 15-20 tools per day for an experienced user, but the merging process minimally takes about an hour per tool.

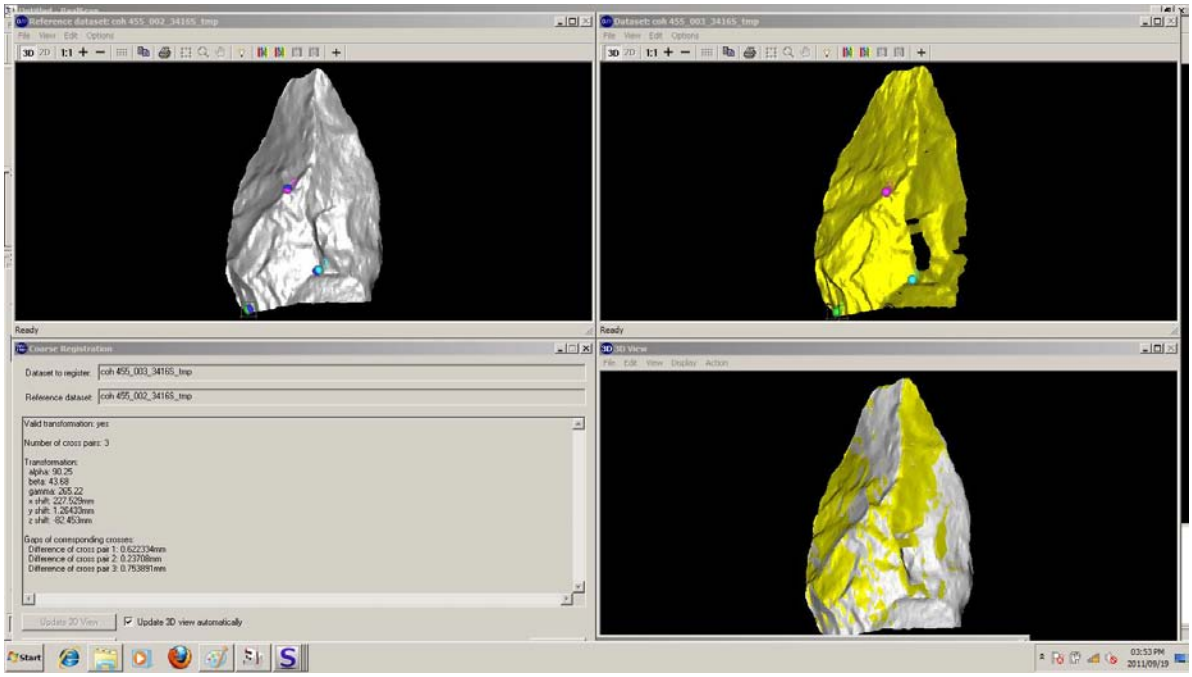

Figure 4: Manual alignment window

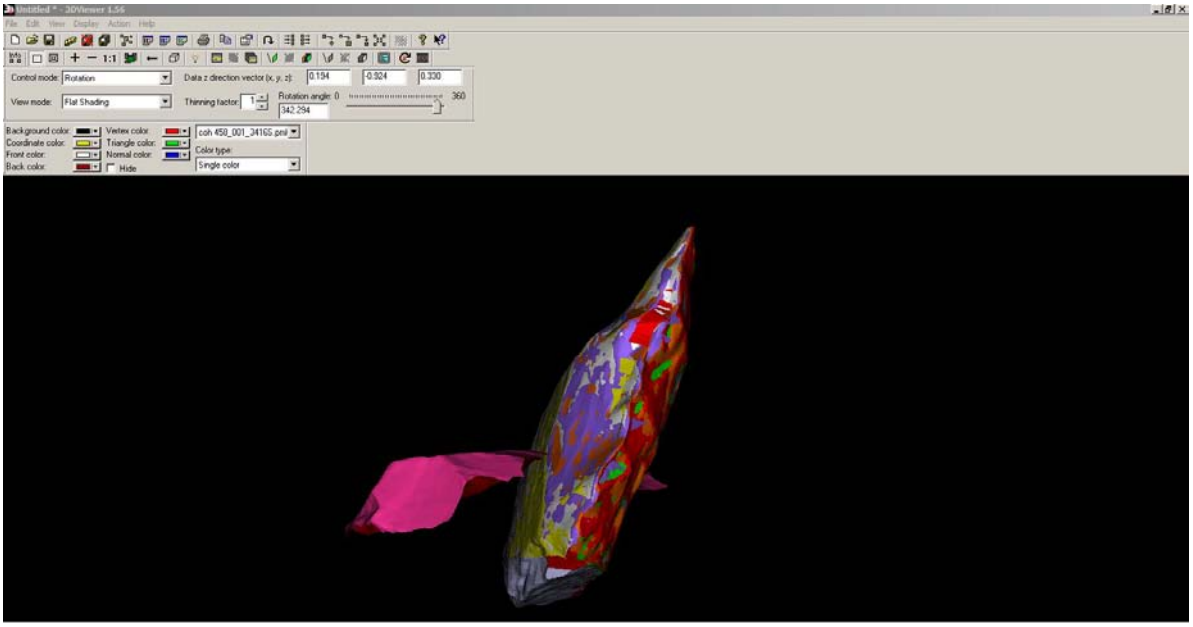

Figure 5: Full pre-merge scan showing incompatible surface

3.2 Editing

The next step in my methodology was the editing of scans to produce measures of surface area and volume for each sector of a given handaxe. This step draws on a more traditional method of measuring handaxes (Roe 1964) but it adds a third dimension using the Avizo 6 programme. This programme allows the user to manipulate objects in 3-D space and is equipped with a multitude of actions useful to any researcher, including two dimensional measures. Avizo 6 provided me with easily extracted measures of volume and area that are otherwise impossible to calculate in the two-dimensional realm. The next section will explain how I did this.

3.2.1 Alignment and Measurements

First, tools are opened and aligned using an xy button that flips the tool into a downward mode with the distal business-end facing downwards. Using the manual rotation wheel located in the lower right of the screen the tool must be aligned upright by 180 degrees. A bounding box is then placed around the tool automatically, and this box defines the maximum dimensions of the tool (maximum width, length, and thickness). This can be seen in Figure 6, showing the tool with bounding box represented as triangular mesh.

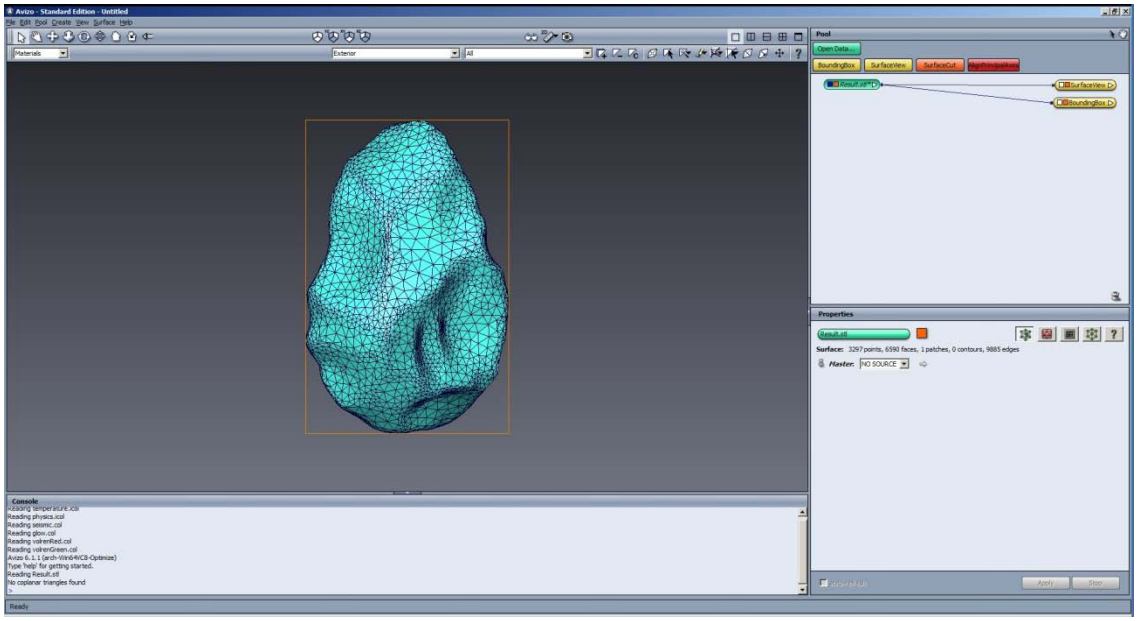

Figure 6: Aligned tool complete with bounding box

A width measurement is done first using a 2D measure (equivalent to using calipers on a real tool). All measurements are reported in mm. Then a mid-point is located using a calculator to divide the tool width by two. From the mid-point a perpendicular angle is created to measure the maximum length, which extends to the top and bottom of the bounding box. Subsequently, maximum length is divided by three to create three proximal-distal arranged sectors that are further subdivided into six sectors by the midline maximum length measurement (see Figure 7). Each sector receives a landmark point to help align the cutting process in the next phase of editing (Figure 7). A thickness measurement is also taken for each tool with the help of the bounding box and recorded in MS Excel, traditionally this is important for calculating degree of refinement for any given tool and can be done in Avizo by simply turning the image sideways (using a shortcut key) and measuring the bounding box. These images are then saved as a network of files so the whole process can be opened at any time before or even during editing.

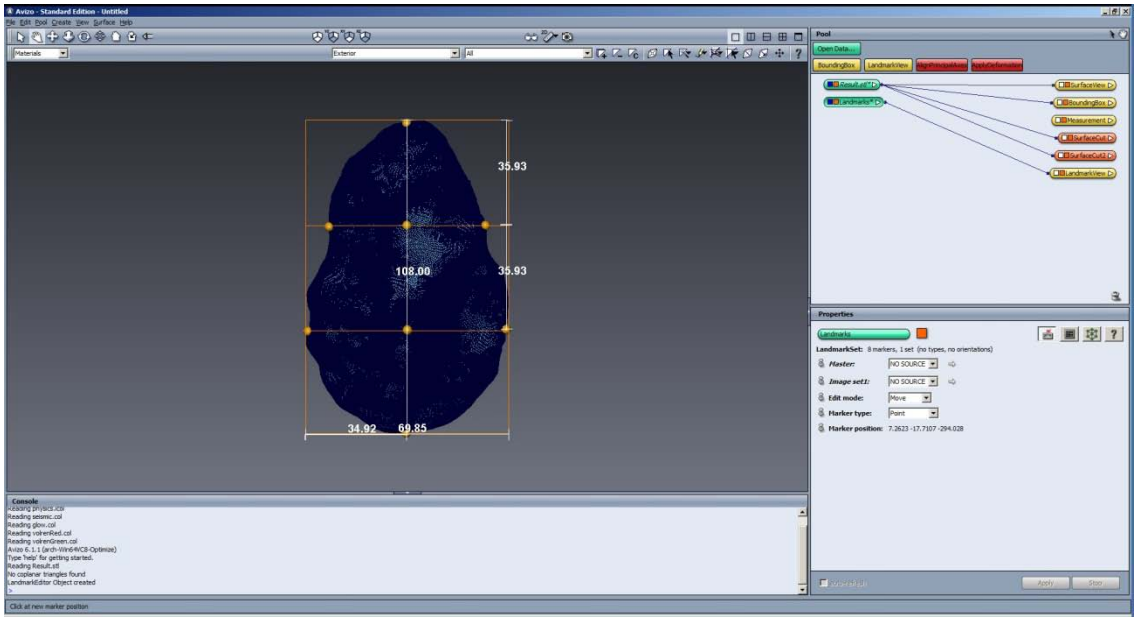

Figure 7: Handaxe scan complete with sectoral divisions, landmarks and bounding box

3.2.2 Division of tools

Next, tools are opened in the measures view. The image quality is refined using a transform editor, effectively making the number of triangles in the surface smaller (i.e., resampling) and increasing the file size. Resampling was performed three times for each tool to improve accuracy at cut surfaces. Otherwise, during 3-D measurements, overlap would have been introduced for triangles of the mesh bordering a cut. Any triangles falling across a cutting line (i.e., introducing overlap) would introduce noise into volume/area measurements (see Figures 6 and 7 for a comparison of an unrefined and refined tool). It is important to note that refining images in this way does not change area or volume measures for the tool, but serves the crucial purpose to protect sectored data from being erroneously skewed.

Next I used a device called a Wacom tablet which is a touch screen stylus tool and a ruler (Figure 8) to divide tools into sectors.

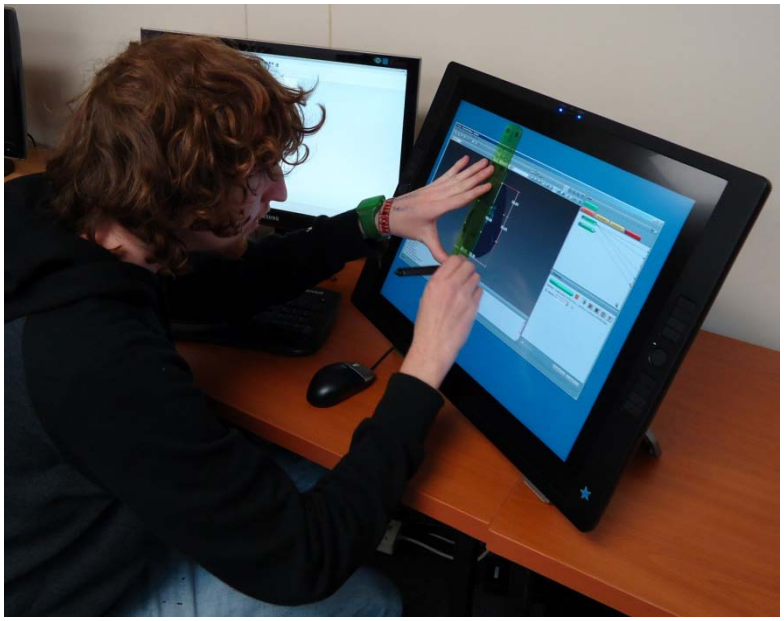

Figure 8: Division of tools into sectors using a Wacom tablet

I started by producing images of the left and right wholes respectively before dividing each side into a further three images namely the tip, medial and base for each side independently thus making up six sectors per tool. Each of the six sectors and the left and right wholes were saved individually and a measure of surface area and volume attached to each sector using a statistical tool incorporated within the Avizo package. All sectors were then saved to a collective network file, and the entire process of division could be opened at any time.

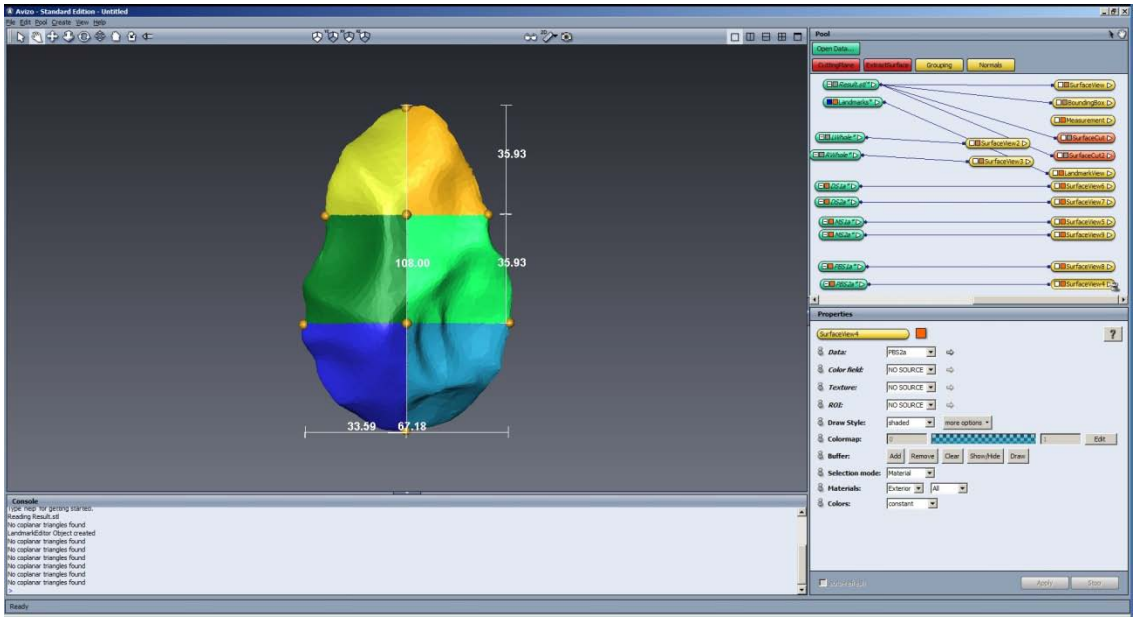

Figure 9: A complete tool divided into 6 sections

3.3 Recording

Tools were labelled according to part of tool and side (as it is in 3-D) thus: DS1a= Distal Sector 1(Left) a (front) and DS2a= Distal Sector 2 (right) a (front), whereas DS1/2b would represent the back of the tool depending on the view in the screen and how it was saved. All tools were saved as (a) which refers to images saved in the default forward view so if future research is done this paper should serve as a reference for interpretation. Other labels used were Left/Right Whole, DS1a/2a, MS1a/2a denotes Medial Sector and lastly PBS1a/2a, which denotes Proximal Basal Sector.*

The editing of a tool measured in this way can take a minimum of about thirty minutes for an experienced researcher.

*Note all tools were analyzed using this method, regardless of whether they were tipped or tipless, and the data for each tool and sector were transferred into an Excel spreadsheet (divided volume/area) so that it could be input by site into the statistical program SPSS for further analysis. Tipless tool values were processed in Excel but not included in this study because the data for the medial sector using this method would be taken as the tip value. Thus this method is limited only to tools that have tips. It is equally important to note that tools were randomly positioned upon initial scanning and tools were not scanned with their dorsal surfaces facing forward, for example. This is a minor limit to this research that should be rectified in future studies.

3.4 Evaluating Symmetry using Statistics

The data presented in this paper was produced using the program IBM SPSS Statistics 19.

The methodology used for this study is one that demonstrates considerable resolution when we consider the symmetry and standardization of any assemblage. In other words, an assemblage can be examined based on the values for whole left and right portions of the handaxe (measured using the longitudinal axis), as well as on a much finer scale by analysing the values for the distal, medial and basal sectors. My results are shown in terms of both area and volume. This is valuable because 2D techniques cannot capture the latter kind of data. For this study, volume seems to be more appropriate because it takes into account the entirety of the tool by including thickness, which area does not.

CHAPTER 4: MATERIALS

4.1 Sample and Raw Materials

For this study a total of 150 handaxes was available yet only 66 handaxes were analysed using the 3-D scanner.

The Rietputs 15 sample was selected randomly and tool attributes were taken from an already existing database created by Kathleen Kuman. The Cave of Hearths handaxes were also selected randomly and raw materials were identified by geologist Professor Terrence McCarthy (University of the Witwatersrand, School of Geosciences). The blank types were classed by Kathleen Kuman in order to regularise this sample with the Rietputs 15 catalogue sample.

This section will discuss the materials and blank types that were analysed for each site; Appendix B provides all the data collected during this study.

4.1.1 Rietputs 15 Raw Materials

For Rietputs, a total of 34 handaxes was analysed. The materials contained in this sample consist primarily of Ventersdorp Lava (n=14) and hornfels (n=16), comprising almost 90% of the total. Chert and quartzite make up the remaining ± 11.7%. These values are summarised in Figure 10 and Table 1.

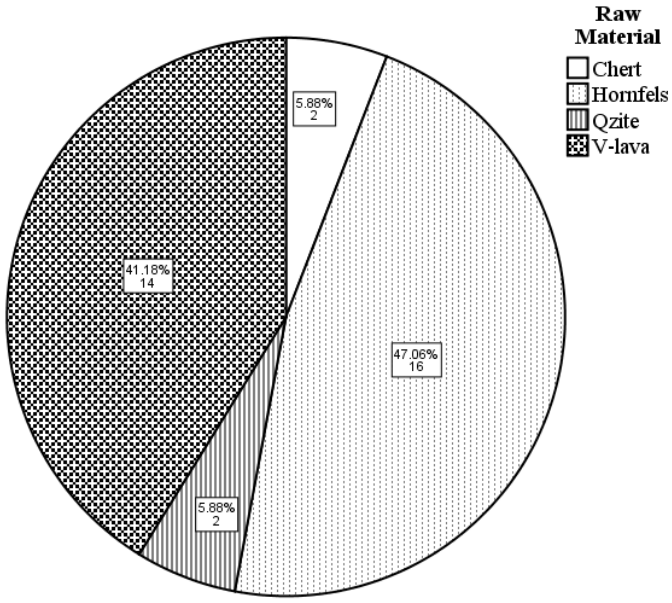

Figure 10: Raw materials at Rietputs 15

Blank Type	Chert	Hornfels	Quartzite	Ventersdorp-Lava	Total	Percentage of total
Flake Incomplete	0	5	1	14	20	58.8%
Chunk	0	0	1	0	1	2.9%
Cobble	1	6	0	0	7	20.5%
Indeterminate	1	5	0	0	6	17.6%
Total	2	16	2	14	34	100%
Percentage of total	5.8%	47%	5.8%	41.1%	100%	

Table 1: The relationship between Raw Material type and Blank Type for the Rietputs 15 site

4.1.2 Rietputs 15 Blank Types

The blank types for Rietputs 15 handaxes consist of: chunks, cobbles, flakes and indeterminates. These labels were employed based on a previous database of Rietputs 15 in order to maintain regularity. The largest portion is flakes (n=20) comprising 58.82% in total although a moderate number of cobbles also exists (n=7 or 20.59%). These values are summarised below in Figure 11 and Table 1.

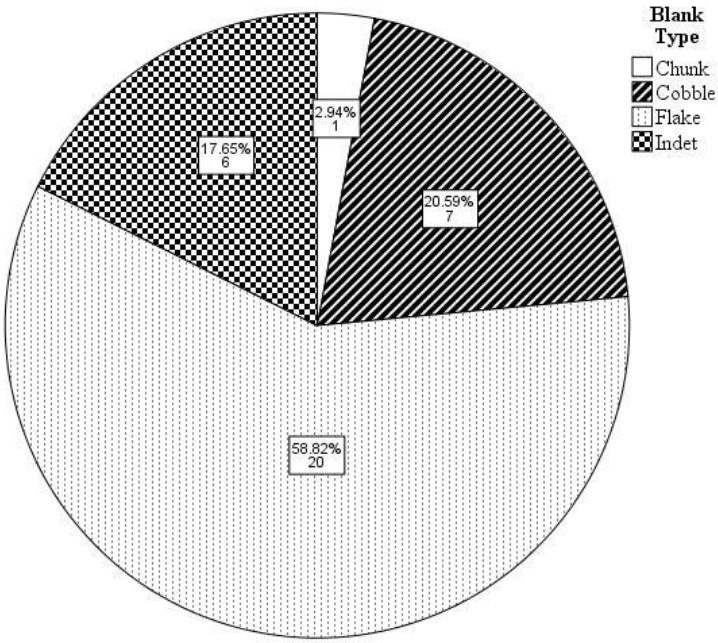

Figure 11: Blank Types at Rietputs 15

4.1.3 Cave of Hearths Raw Materials

For the Cave of Hearths a total of 32 handaxes was examined. There were seven different raw materials in this sample as opposed to Rietput's four; they are classed below in Figure 12 and Table 2. Quartzite dominates this sample (n=14) comprising 44% of the total. Dolerite (n=6) also makes up a significant portion of the sample, followed closely by quartz (n=5) and shale (n=3) which make up a further 40% of the total types.

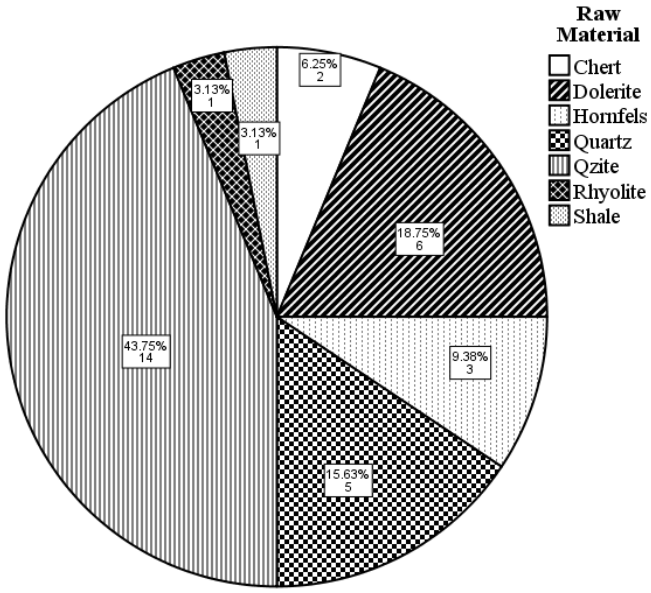

Figure 12: Raw materials at the Cave of Hearths

Blank Type	Chert	Dolerite	Hornfels	Rhyolite	Shale	Quartzite	Quartz	Total	Percentage of total
Flake Incomplete	0	0	0	0	0	4	0	4	12.5%
End struck flake	2	0	2	0	0	4	1	9	28.1%
Side struck flake	0	3	0	0	0	3	4	10	31.2%
Corner struck flake	0	0	0	0	0	1	0	1	3.1%
Slab	0	0	0	0	1	0	0	1	3.1%
Cobble	0	0	0	1	0	0	0	1	3.1%
Indeterminate	0	3	1	0	0	2	0	6	18.7%
Total	2	6	3	1	1	14	5	32	100%
Percentage of total	6.2%	18.7%	9.3%	3.1%	3.1%	43.7%	15.6%	100%	

Table 2: The relationship between Raw Material type and Blank Type for the Cave of Hearths site

4.1.4 Cave of Hearths Blank Types

The blank types for the Cave of Hearths include: Corner Struck Flakes, End Struck Flakes, Side Struck Flakes, Indeterminate Flakes (flaking axis not visible), Indeterminate, Slabs, and Split Cobbles. The most dominant blank type is the End- Struck Flake (n=9) comprising 28% of the sample followed closely by Flakes and Indeterminates (n=8 for both), which make up 25% of the assemblage each. The values are shown in Figure 13 and Table 2. Flaking axis for Cave of Hearths was determined for comparative purposes within the sub-types, which will be discussed in due course.

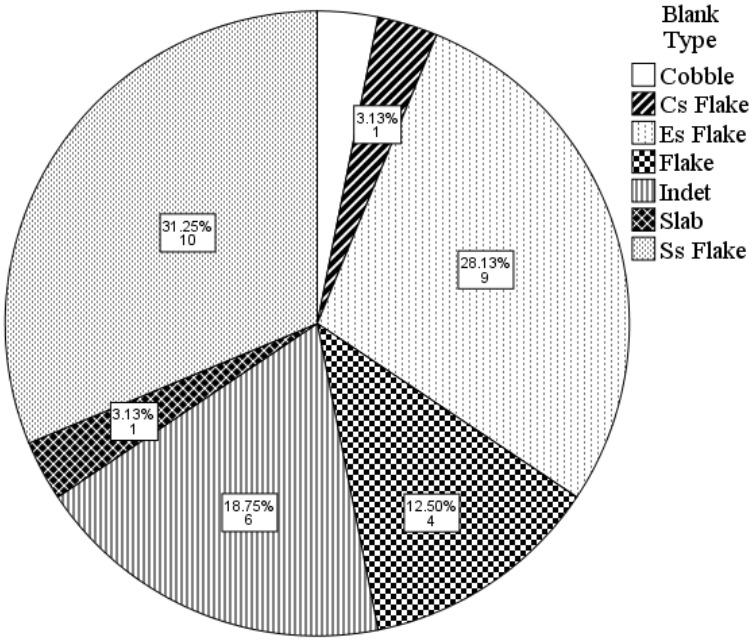

Figure 13: Blank Types at the Cave of Hearths

CHAPTER 5: RESULTS

5.1 General

All data collected during this study can be referred to in the Appendices. Mean sector values reported in Tables 15 through 20 are given in percentages, which are easier to interpret than the large absolute values. For ease of reference, all figures and tables have been placed at the end of this chapter (pg 32-44).

5.2 Results

In Chapter 2, I stated that symmetry is thought to increase over time, and I aimed to test to what degree this is consistent with tools from my two sites of interest. In statistical terms, my null hypothesis (H_o) was that: the variables being tested (e.g., left and right wholes) are not associated. This implies little or no symmetry. My alternative hypothesis (H_A) was that: variables being investigated (e.g., left and right wholes) are associated. This would imply that symmetry exists, and a correlation value would give some indication of how strong this association could be. The second objective was to determine what factors, if any, could influence symmetry.

Figures 14 and 15, which are complementary to Tables 3 and 4, illustrate Rietputs 15 (early Acheulean) and Cave of Hearths (later Acheulean) volume plots, respectively. Figures 16 and 17, which are complementary to Tables 5 and 6, illustrate the same, but in terms of area. Each scatter plot depicts the relationship between one side/sector and its counterpart, the line indicated in each graph is a reference line with equation: $y = 1 * x + 0$. Each point corresponds to a combination of left and right values for specific tools. The closer a point is to the reference line, the more symmetrical the values are (y = x).

This relationship can be quantified mathematically by using the Pearson Correlation Coefficient (*r*). It is shown in the tables below each graph. The coefficient is useful for showing the relationship between two variables: a correlation of 1 would represent a perfect association, whereas zero would represent that no association exists (Minium 1978). In order

to make sure the Pearson Correlation Coefficient was suitable for this study I tested my data using the Komogrov Smirnov (K-S) test to assess variable distributions versus normal distributions. I found no differences between them thus, leading me to use the Pearson Correlation as opposed to a non-parametric alternative

According to Minium (1978: 143): ‘’the sign of the coefficient may be positive or negative. A positive value of *r* indicates that there is a high tendency for high values of one variable (X) to be associated with high values of the other variable (Y), and low values of one to be associated with low values of the other.’’ A negative value for *r* means that high values of one variable are associated with low values of the other, and vice versa. It is important to note that negative and positive values merely reflect differences in the direction of an association rather than the strength of association (Minium 1978).

We would expect a graph showing a perfect $r = 1$ value to have points distributed along the line and no error resulting in points clustering off the line to a variable degree.

The second important value when interpreting the tables given below is the ‘Sig. one/two tailed value’. This value is also known as the *P* value, and is a measure of significance. In standard scientific research, the general practise when performing statistical testing is to reject H_o when the significance value (p) is below a chosen value. Typically this value is chosen to be equal to/less than 0.05 or 0.01. When H_o is rejected, the alternative hypothesis (H_A) is accepted. All statistical significance in this study is determined by using a significance value (P) of 0.05.

5.3 Interpretation

Figures 14 and 15 illustrate left and right side volumes of handaxes from Rieputs 15 and Cave of Hearths, respectively, Side volumes are highly associated on their own, and also individually at Rietputs 15 versus the Cave of Hearths. Their correlation coefficients are close to 1 with Rietputs at 0.859 and Cave of Hearths at 0.870 for side volume and 0.954 and 0.960, respectively for side area (see Figures 16 and 17). Results for both sites are statistically significant, meaning H_o is rejected. For both side area and side volume, Cave of Hearths has a stronger correlation (which we would expect because it is later Acheulean). Thus, as one side

increases so does its counterpart. Based on this, we could regard Cave of Hearth's tools as more symmetrical than Rietputs (in terms of left and right). However, the difference in value between the two (i.e., strength of correlations) is extremely close, A larger sample size could be useful to further draw out these apparent differences.

5.3.1 The Coefficient of Variation (CV)

The Coefficient of Variation (CV) is statistically a normalized measure of dispersion that proved useful to this study with regards to analysing the sector data. The CV is defined as the ratio of the standard deviation to the mean: $C_v =$. Larger CVs indicate more dispersion around the mean (i.e., lots of variability in the sample), while lower CVs indicate less dispersion around the mean (i.e., less variability in the sample).

5.3.2 Interpretation

See the Appendices for complete CV tables that show all variables measured.

Tables 15 through 18 represent CV and means for each site.

Means and CVs of linear measures (i.e. width, length and thickness) are very similar across assemblages. Cave of Hearths shows better control of shape based on the fact that these CV values are more consistent than those for Rietputs (around 0.21-22). The Cave of Hearths handaxes also have longer mean lengths than Rietputs.

By examining mean values and CVs of area and volume for both sites, it is clear that left and right sides are very symmetrical in both cases, and that the differences in variability between them are minimal. However, when looking at sector data, substantial variability in the distal ends of both assemblages compared with the medial and proximal sectors of the tool is apparent. In the case of area values, the medial and proximal (base) sectors are less variable with almost perfect symmetry displayed (see Tables 15 to 18).

It should be kept in mind that volumes and their CVs are generally larger than areas and their CVs because of the inclusion of thickness in the former (i.e., area scatter plots will appear more clustered because thickness has not been accounted for), but regarding our interpretation this is a negligible difference. It is also interesting to note that in terms of

volumes, a single edge for both assemblages displays the highest variation in all sectors of the tools, especially the tip. It is reasonable to assume from this data that the distal sector as well as one edge of the tool was the main focal point during manufacture and use. Unfortunately the first face of a tool to be scanned was randomly positioned, rather than having the dorsal face of the tool (if made on a flake blank) scanned first. This has made it impossible to designate specific sides of reference at this point in time. Future work will need to be employed to achieve this.

The Cave of Hearths seems to exhibit a higher degree of variability for all sectoral divisions of a handaxe, but when we look at only left and right it shows a higher degree of symmetry between the two sides. This is probably due to continuous edge re-sharpening as a result of use, coupled with increased cognitive understanding leading to greater control of form over time (McNabb 2004). Rietputs 15 handaxes are generally quite robust and often pick-like, and it is probable that the tip was the primary emphasis (Kuman & Gibbon, in press). We can see this by looking at Tables 15 - 18 because the tip is more variable than the rest of the tool. However, Cave of Hearth's handaxes are less pick-like and more emphasis was apparently placed on the entire edge of the tool and not only the tip.

5.3.3 Blank Type and Symmetry

With visual study of the Cave of Hearths handaxes, it was easy to distinguish two groups of blank types--end-struck and side-struck. When we compare means and CVs of these two groups (Tables 19 and 20), we can see that side-struck pieces seem to exhibit the least amount of variation in symmetry between left and right sides, as well as in linear dimensionality (length, width, thickness). In terms of sector analysis, both groups in the Cave of Hearths sample still exhibit similar variations, but overall side-struck pieces seem to produce more symmetric handaxes. The reason could be that the broad striking platforms of side-struck blanks allow more opportunity to remove thickness, while end-struck blanks are more compromised.

5.3.4 Raw Material and Symmetry

Figures 20 and 21 show a more simplified left/right breakdown for both sites by their most dominant raw materials (i.e., dolerite and quartzite). The *r* and *P* values for material-specific side correlations are given in Tables 11 to 14. All comparisons have very strong correlations.

5.4 Volume Scatterplots

5.4.1 Rietputs 15 Volume

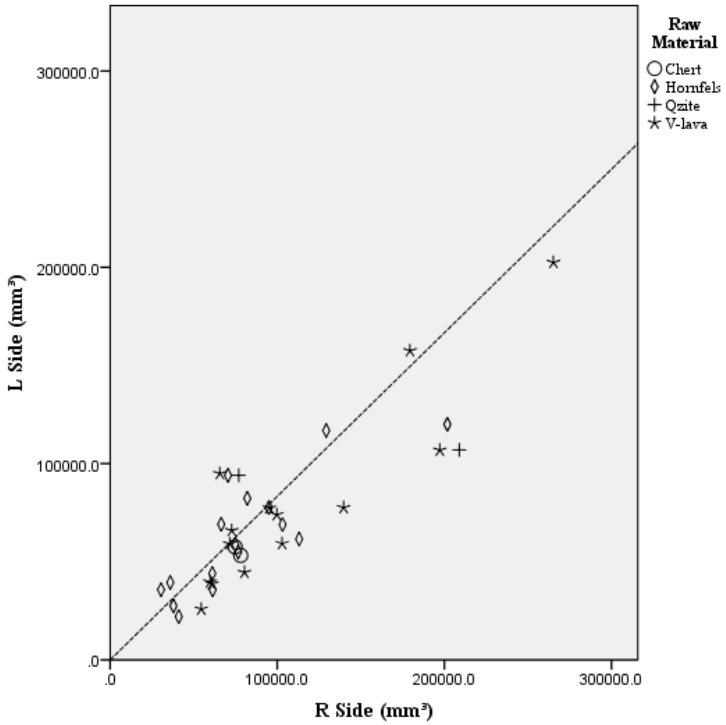

Figure 14: Volume scatterplot of left and right sides for Rietputs 15 handaxes

Correlation between volumes of left and right sides of Rietputs 15 handaxes

		L Whole	R Whole
L Whole	Pearson Correlation	1	.859**
	Sig. (2-tailed)		.000
	N	34	34
R Whole	Pearson Correlation	.859**	1
	Sig. (2-tailed)	.000	
	N	34	34

**. Correlation is significant at the 0.01 level (2-tailed).

Table 3: Pearson Correlation for volumes of left and right sides of Rietputs 15 handaxes

5.4.2 Cave of Hearths Volume

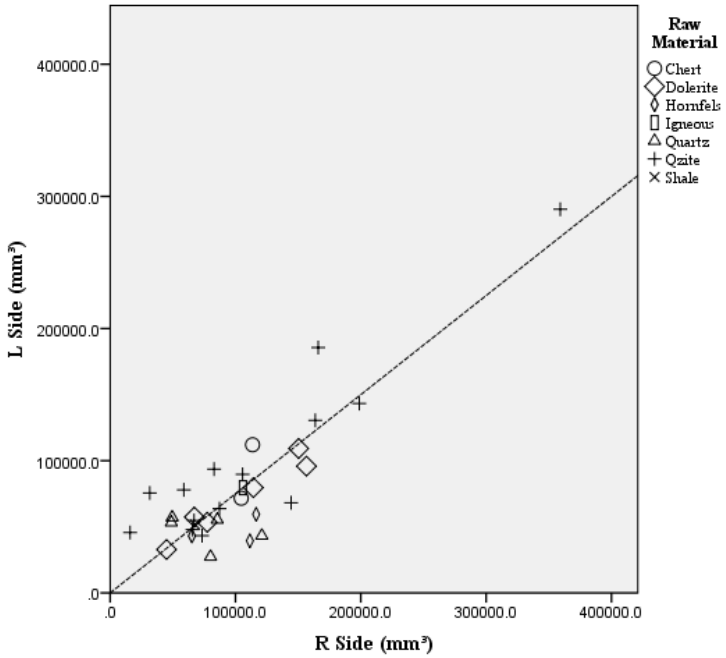

Figure 15: Volume scatterplot of left and right sides for the Cave of Hearths handaxes

Correlation between volumes of left and right sides of the Cave of Hearths handaxes

		L Whole	R Whole
L Whole	Pearson Correlation	1	.870**
	Sig. (2-tailed)		.000
	N	32	32
R Whole	Pearson Correlation	.870**	1
	Sig. (2-tailed)	.000	
	N	32	32

**. Correlation is significant at the 0.01 level (2-tailed).

Table 4: Pearson Correlation for volume of left and right sides of the Cave of Hearths handaxes

5.5 Area Scatterplots

5.5.1 Rietputs 15 Area

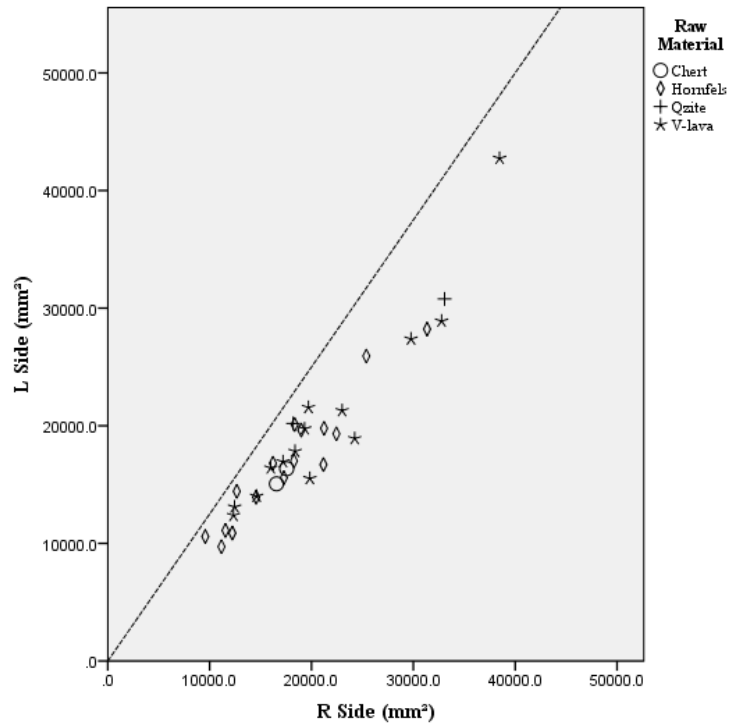

Figure 16: Area scatterplot of left and right sides for Rietputs 15 handaxes

Correlation between areas of left and right sides of Rietputs 15 handaxes

		L Whole	R Whole
L Whole	Pearson Correlation	1	.954**
	Sig. (2-tailed)		.000
	N	34	34
R Whole	Pearson Correlation	.954**	1
	Sig. (2-tailed)	.000	
	N	34	34

**. Correlation is significant at the 0.01 level (2-tailed).

Table 5: Pearson Correlation for area of left and right sides of Rietputs 15 handaxes

5.5.2 Cave of Hearths Area

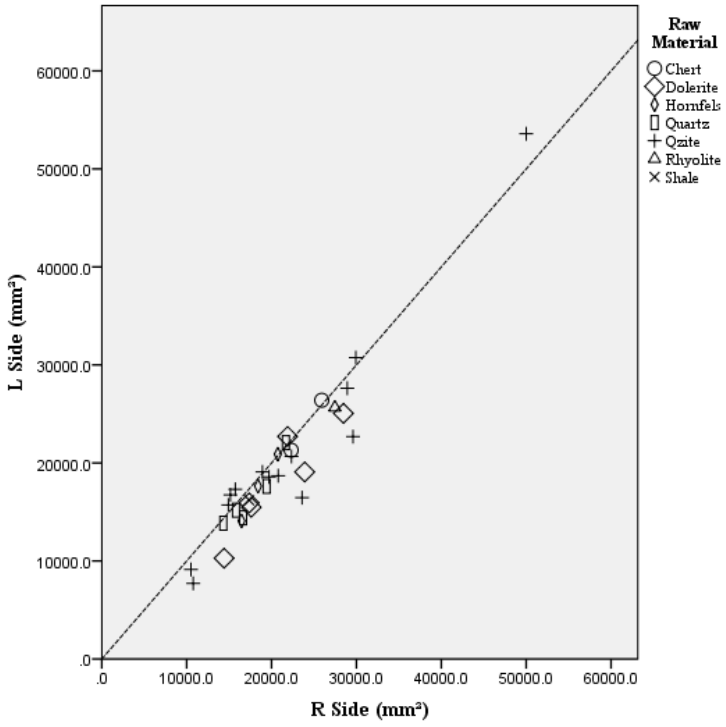

Figure 17: Area scatterplot of left and right sides for the Cave of Hearths handaxes

Correlation between areas of left and right sides of Cave of Hearths handaxes

		L Whole	R Whole
L Whole	Pearson Correlation	1	.960**
	Sig. (2-tailed)		.000
	N	32	32
R Whole	Pearson Correlation	.960**	1
	Sig. (2-tailed)	.000	
	N	32	32

**. Correlation is significant at the 0.01 level (2-tailed).

Table 6: Pearson Correlation for area of left and right sides for Cave of Hearths handaxes

5.6 Raw Material Scatterplots

5.6.1 Rietputs 15 Area

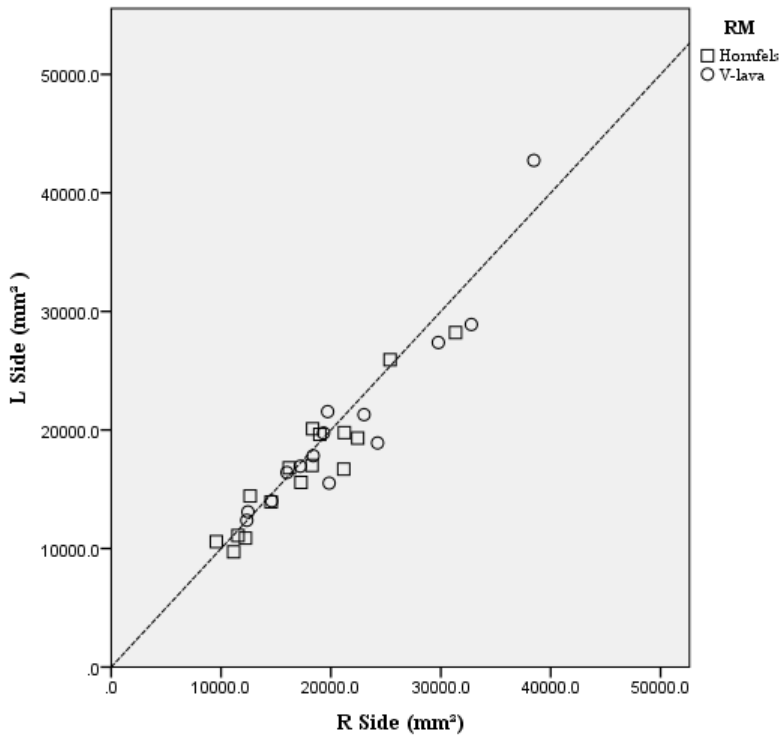

Figure 18: Area scatterplot of left and right sides of Rietputs 15 handaxes by dominant raw material

Correlation between area of left and right sides of Rietputs 15 handaxes for hornfels

		L Whole	R Whole
L Whole	Pearson Correlation	1	.952**
	Sig. (2-tailed)		.000
	N	16	16
R Whole	Pearson Correlation	.952**	1
	Sig. (2-tailed)	.000	
	N	16	16

**. Correlation is significant at the 0.01 level (2-tailed).

Table 7: Pearson correlation for area of left and right sides for Rietputs 15 handaxes for hornfels

Correlation between area of left and right sides of Rietputs 15 handaxes for Ventersdorp Lava

		L Whole	R Whole
L Whole	Pearson Correlation	1	.949**
	Sig. (2-tailed)		.000
	N	14	14
R Whole	Pearson Correlation	.949**	1
	Sig. (2-tailed)	.000	
	N	14	14

**. Correlation is significant at the 0.01 level (2-tailed).

Table 8: Pearson correlation for area of left and right sides for Rietputs 15 handaxes for ventersdorp lava

5.6.2 Rietputs 15 Volume

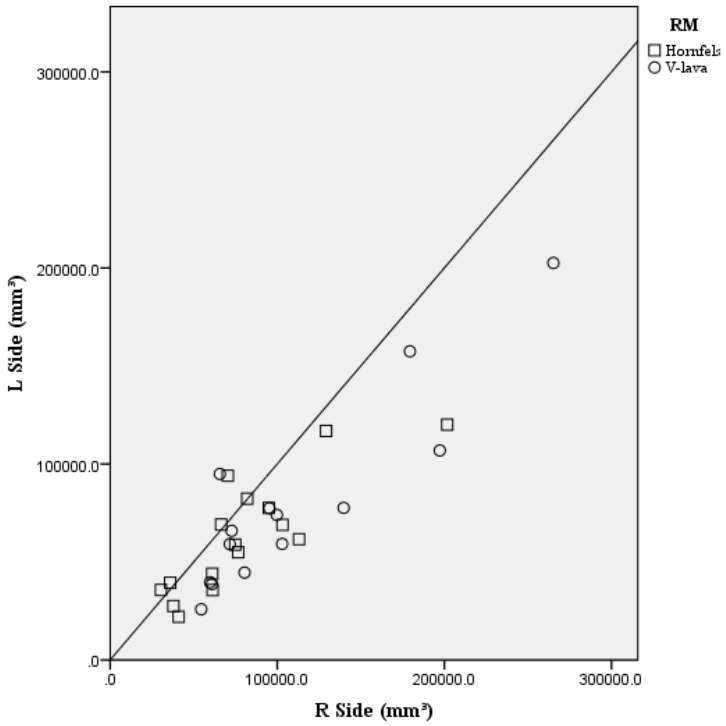

Figure 19: Volume scatterplot of right and left sides of Rietputs handaxes by dominant raw material

Correlation between volumes of left and right sides of Rietputs 15 handaxes for hornfels

		L Whole	R Whole
L Whole	Pearson Correlation	1	.833**
	Sig. (2-tailed)		.000
	N	16	16
R Whole	Pearson Correlation	.833**	1
	Sig. (2-tailed)	.000	
	N	16	16

**. Correlation is significant at the 0.01 level (2-tailed).

Table 9: Pearson Correlation for volume of left and right sides for Rietputs 15 handaxes for hornfels

Correlation between volumes of left and right sides of Rietputs 15 handaxes for ventersdorp lava

		L Whole	R Whole
L Whole	Pearson Correlation	1	.899**
	Sig. (2-tailed)		.000
	N	14	14
R Whole	Pearson Correlation	.899**	1
	Sig. (2-tailed)	.000	
	N	14	14

**. Correlation is significant at the 0.01 level (2-tailed).

Table 10: Pearson Correlation for volume of left and right sides for Rietputs 15 handaxes for ventersdorp lava

5.6.3 Cave of Hearths Area

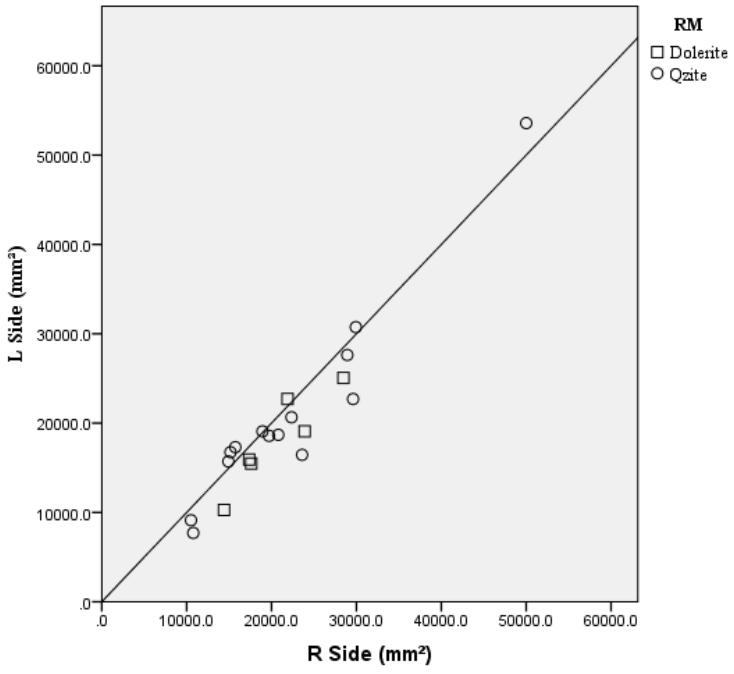

Figure 20: Area scatterplot of left and right sides of Cave of Hearths handaxes by dominant raw material

Correlation between area of left and right sides of Cave of Hearths handaxes for Dolerite

		L Whole	R Whole
L Whole	Pearson Correlation	1	.924**
	Sig. (2-tailed)		.008
	N	6	6
R Whole	Pearson Correlation	.924**	1
	Sig. (2-tailed)	.008	
	N	6	6

**. Correlation is significant at the 0.01 level (2-tailed).

Table 11: Pearson Correlation for area of left and right sides for Cave of Hearths 15 handaxes for dolerite

Correlation between area of left and right sides of Cave of Hearths handaxes for quartzite

		L Whole	R Whole
L Whole	Pearson Correlation	1	.963**
	Sig. (2-tailed)		.000
	N	14	14
R Whole	Pearson Correlation	.963**	1
	Sig. (2-tailed)	.000	
	N	14	14

**. Correlation is significant at the 0.01 level (2-tailed).

Table 12: Pearson correlation for area of left and right sides for Cave of Hearths handaxes for quartzite

5.6.4 Cave of Hearths Volume

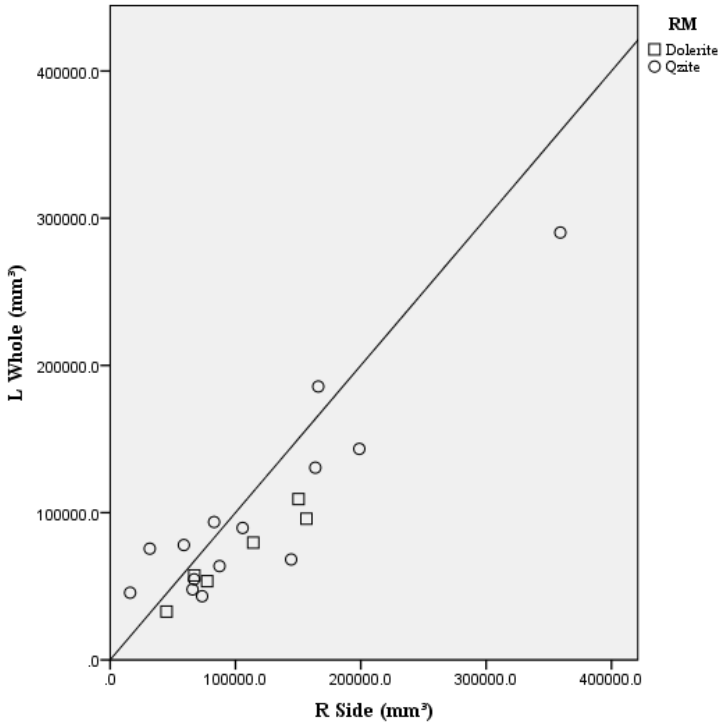

Figure 21: Volume scatterplot of left and right sides of Cave of Hearths handaxes by dominant raw material

Correlation between volume of left and right sides of Cave of Hearths handaxes for dolerite

		L Whole	R Whole
L Whole	Pearson Correlation	1	.972**
	Sig. (2-tailed)		.001
	N	6	6
R Whole	Pearson Correlation	.972**	1
	Sig. (2-tailed)	.001	
	N	6	6

**. Correlation is significant at the 0.01 level (2-tailed).

Table 13: Pearson Correlation for volume of left and right sides for Cave of Hearths 15 handaxes for dolerite

Correlation between volume of left and right sides of Cave of hearths handaxes for quartzite

		L Whole	R Whole
L Whole	Pearson Correlation	1	.921**
	Sig. (2-tailed)		.000
	N	14	14
R Whole	Pearson Correlation	.921**	1
	Sig. (2-tailed)	.000	
	N	14	14

**. Correlation is significant at the 0.01 level (2-tailed).

Table 14: Pearson Correlation for volume of left and right sides for Cave of Hearths handaxes for quartzite

5.7 Coefficient of Variation Tables

5.7.1 Area

	Max Width (cm)	Max Length (cm)	Max Thickness (cm)	Left Side (mm^2)	Right Side (mm^2)	Distal Left (%)	Distal Right (%)	Medial Left (%)	Medial Right (%)	Proximal Left (%)	Proximal Right (%)
Mean	60.4	122.6	46.54	18787.1	19583.15	10.86	12.51	19.84	20.4	18.3	18.08
Standard Deviation	10.17	29.57	9.5	6801.44	6923.52	2.98	2.75	1.2	1.56	2.5	2.65
CV	**0.16**	**0.24**	**0.20**	**0.36**	**0.35**	**0.27**	**0.21**	**0.06**	**0.07**	**0.13**	**0.14**

Table 15: Coefficient of Variation for linear measurements and area in the Rietputs 15 assemblage

	Max Width (cm)	Max Length (cm)	Max Thickness (cm)	Left Side (mm^2)	Right Side (mm^2)	Distal Left (%)	Distal Right (%)	Medial Left (%)	Medial Right (%)	Proximal Left (%)	Proximal Right (%)
Mean	59.86	128.12	45.11	19639.89688	20971.74	9.3875	13.34	19.75	20.26	18.85	18.38
Standard Deviation	12.81	28.88	10.01	8084.37	7451.63	3.09	2.53	1.09	1.2	2.79	1.89
CV	**0.21**	**0.22**	**0.22**	**0.41**	**0.35**	**0.32**	**0.18**	**0.05**	**0.05**	**0.14**	**0.10**

Table 16: Coefficient of Variation for linear measurements and area in the Cave of Hearths assemblage

5.7.2 Volume

	Max Width (cm)	Max Length (cm)	Max Thickness (cm)	Left Side (mm^3)	Right Side (mm^3)	Distal Left (%)	Distal Right (%)	Medial Left (%)	Medial Right (%)	Proximal Left (%)	Proximal Right (%)
Mean	60.4	122.6	46.54	71882.81	96004.14	8.21	12.31	13.42	19.17	21.51	25.36
Standard Deviation	10.17	29.57	9.5	38258.8	55102.64	3.97	4.34	3.74	4.13	6.16	5.53
CV	**0.16**	**0.24**	**0.20**	**0.53**	**0.57**	**0.48**	**0.35**	**0.27**	**0.21**	**0.28**	**0.21**

Table 17: Coefficient of Variation for linear measurements and volume in the Rietputs 15 assemblage

	Max Width (cm)	Max Length (cm)	Max Thickness (cm)	Left Side (mm^3)	Right Side (mm^3)	Distal Left (%)	Distal Right (%)	Medial Left (%)	Medial Right (%)	Proximal Left (%)	Proximal Right (%)
Mean	59.86	128.12	45.11	79115	103155.97	7.54	12.35	14.43	18.9	21.98	24.81
Standard Deviation	12.81	28.88	10.01	51638.15	63143.22	4.28	4.46	5.34	5.62	7.07	6.27
CV	**0.21**	**0.22**	**0.22**	**0.65**	**0.61**	**0.56**	**0.36**	**0.37**	**0.29**	**0.32**	**0.25**

Table 18: Coefficient of Variation for linear measurements and volume in the Cave of Hearths assemblage

5.7.3 Cave of Hearths Symmetry and Blank Type.

	Max Width (cm)	Max Length (cm)	Max Thickness (cm)	Left Side (mm3)	Right Side (mm3)	Distal Left (%)	Distal Right (%)	Medial Left (%)	Medial Right (%)	Proximal Left (%)	Proximal Right (%)
Mean	65.8	129.2	46.2	89680.6	108934.7	8.1	10.8	12.9	17.8	24.9	25.2
Standard Deviation	17.6	29	10.4	78087.2	98225.3	4.1	4.1	4.9	5.2	7.1	6.9
CV	**0.26**	**0.22**	**0.22**	**0.87**	**0.90**	**0.50**	**0.37**	**0.37**	**0.29**	**0.28**	**0.27**

Table 19: Coefficient of Variation for linear measurements and volume of End Struck Pieces for the Cave of Hearths sub-sample (n=9)

	Max Width (cm)	Max Length (cm)	Max Thickness (cm)	Left Side (mm3)	Right Side (mm3)	Distal Left (%)	Distal Right (%)	Medial Left (%)	Medial Right (%)	Proximal Left (%)	Proximal Right (%)
Mean	56.7	134.8	44.8	84029.4	114785.5	8.23	13.6	14.8	21.1	17.7	24.4
Standard Deviation	10.4	21.3	7.5	49538.8	45794.3	4.7	4.3	5	5.2	4.8	7.3
CV	**0.18**	**0.15**	**0.16**	**0.58**	**0.39**	**0.57**	**0.31**	**0.33**	**0.24**	**0.27**	**0.29**

Table 20: Coefficient of Variation for linear measurements and volume of side-struck pieces for the Cave of Hearths sub-sample (n=10)

CHAPTER 6: DISCUSSION

6.1 Discussion

Using this method, symmetry can clearly be quantified in terms of the tool as a whole and within separate divisions. Both aspects are equally important when we attempt to interpret and compare the Cave of Hearths and Rietputs 15 handaxes.

McNabb *et al.* (2004) explain that very little absolute symmetry exists for the Cave of Hearth's Large Cutting Tools because many of the tools display such variable tips. They explain that symmetry only rarely occurred in isolated sections of the tools and concluded that because of the large amount of variation in the tools the presence of symmetry could be taken as either chance or could have been produced when a knapper was trying to produce a more elongated tip. Statistically, however, strong correlations in this study support the presence of very good symmetry in complete handaxes at the cave (r = 0.870 for volume, r =0.960 for area). This study was mathematically based, in contrast with the previous subjectively scrutinized method. Results of the present study do not suggest that McNabb *et al's*. (2004) research is flawed, but simply that the three-dimensional quantification of data may lead to more accurate interpretations of a given assemblage. In this study it is shown that both sites display similar degrees of symmetry on a holistic level, which may seem surprising given the extensive time span between both sites. However, the fact that the values for the Early Acheulean sample from Rietputs 15 are also fairly high suggests that the convergent template of a handaxe, by its very nature, puts constraints on the bilateral dimensions for this special tool type. Overall for the Rietputs specimens, correlations were also strong: r = 0.859 for volume, and r = 0.954 for area. If blank type is then considered, the lava specimens exhibit an even higher value (r = 0.899 v. 0.833 for hornfels). The explanation for this difference may be explained by blank type. Lava handaxes in this assemblage are always made on flake blanks, whereas hornfels handaxes are made on both cobbles and flakes and thus they reflect more inherent variability (K. Kuman, pers. comm.).

The breakdown of these symmetries into sectors is equally important because it allows us to focus specifically on what areas of a tool were most significant to their manufacturers.

It is plainly shown that the distal sector in all cases of the aforementioned results is the most varied area of these handaxes (even when overall near-perfect left/right symmetry exists). This variability is also something that McNabb *et al.* (2004) stress quite highly in their paper, and their analysis of the tip forms is quite rigorous as a result. They also suggest that most tips at the Cave of Hearths are asymmetrical or 'bent' and that the purpose of this attribute is not easily understood. In light of this observation my study proposes that the use of sector analysis helps us recognise patterns relating to the whole tool rather than just one aspect. The results of this study show that there is a slight trend for the one side of all sectors to be more varied than the other, and in future it will be determined if this is consistent when specimens are scanned first for the dorsal face, which may tend to have more shaping scars. It could be suggested that handaxes at the Cave of Hearths were made in such a way that a unilateral use was being implemented, as opposed to an ambilateral use. The trend noted here also occurs for Rietputs 15, although the CV values for just the tips at both sites show that the variation is larger in the Cave of Hearths assemblage. This could be a functionally driven result. Schick & Toth (1995) and Domínguez-Rodrigo & de la Torre (2002) suggest that the edge of a handaxe would have been its most important feature for cutting, scraping or butchery; Posnansky (1959) also explains that if one side is more asymmetric then we would expect more weight to exist behind the cutting edge of the tool thus increasing its efficacy.

Based on these results it is possible to couple the differences in morphology for both these sites with a number of factors. It was stated previously that Rietputs 15 handaxes are generally quite robust in terms of tip (Kuman and Gibbon, in press) possibly because they were being used for hacking or digging up roots (Kuman pers. comm.). This could account for the greater asymmetry in the distal region of the Cave of Hearths sample if this later Acheulean assemblage was more dedicated to cutting functions. Or it could simply be that the producers could not efficiently shape flatter tips at Rietputs 15 at the time. Both sites have handaxes that are made on fine-grained material so it is feasible that the level of technical control at the Cave of Hearths was overall greater and the degree of re-sharpening may have been of more importance when we consider what activities handaxes were necessary for at the cave. It is possible that the greater variation in tips at the Cave of Hearths was because an emphasis was being placed on the tips for scraping or skinning and/or cutting (Domínguez-Rodrigo & de la Torre 2002, Schick & Toth 1995, Posnanksy 1959). In either case the difference seems to be functionally based.

By looking at the mean linear dimensions for the Cave of Hearths we can see that handaxes are only marginally longer than those at Rietputs 15 and are also thinner. Thinner handaxes may have improved cutting ability. This study could not address re-sharpening, but it should be considered in the future.

Blank type also seems to have played an interesting role in handaxe symmetry at the Cave of Hearths. Side-struck pieces are thinner, longer and less variable in terms of total symmetry than the dominant blank type, end-struck flakes. Although the trend for one side to be more varied than its counterpart holds for both types of blank, it would seem that, overall, side-struck pieces are the least variable and are more symmetric.

6.2 The Question of Handedness.

Posnansky (1959) explains that handedness is something that has been addressed in lithic studies but not much research has been done recently and previous studies were limited, isolated cases. In most circumstances modern human proxies are used to create the statistics that suggest whether a population is mainly left- or right-handed. This could be something to further investigate using the type of methodology presented in this paper and would be interesting when combined with a larger sample size than that which was used for this study.

CHAPTER 7: CONCLUSION

This study has described a few interesting things about Rietputs 15 and Cave of Hearths handaxes. First, it has quantifiably measured the correlation between left and right sides for each site and shown a good measure of symmetry for each: for the Cave of Hearths, $r = 0.870$ for volume, $r = 0.960$ for area; for Rietputs, $r = 0.859$ for volume, and $r = 0.954$ for area. Secondly, using my methodology I was able to assess variability in tools sector by sector, finding that that variabililty was greatest in the tips for both sites. This permitted some inferences about function. Thirdly, by looking at the raw material and blank data, I was able to speculate that side-struck tools were easier to make symmetrical than end-struck pieces.

As our own minds are constantly working to try to make our lives easier by producing remarkable new technologies, it seems only suitable to use the technology available to us to try and decipher the true beginnings of man and his/her experiments with the earliest stone tools of the past. The importance and use of three-dimensional analyses to archaeological assemblages of the Acheulean was presented in this dissertation and has thus led to several interesting conclusions. The data presented by this paper was useful in producing quantitative measures of symmetry for both Rietputs 15 (early Acheulean) and the Cave of Hearths (later Acheulean), which were previously unaccounted for at these sites before now. The second major finding is that the tip is the most variable portion of the tools at both sites, which could be related to function in some way. A third primary conclusion that we could draw from this analysis is that blank type and raw material play some role in defining symmetry.

The benefits of using three-dimensional techniques for analysis can hardly be downplayed. 3D scanning is a simple procedure and the data produced can be stored indefinitely quite literally in one's pocket. Scans can be transmitted between research groups and across borders with the touch of a button and equally so; the more literature that is produced on three-dimensional analysis can only strengthen how it is used and understood. This study aimed to do just that, by formulating an entirely new way of analysing and aligning Large Cutting Tools, more specifically handaxes. The alignment of tools using this methodology is important because the computer program Avizo 6 works with the exact dimensions of the tool at hand in a way that manual alignment can take seconds thereafter. The study described here minimizes user biases and lets the tool speak for itself so to speak. Although I realize that there are problems in how 3D studies are carried out, for example how tools are aligned, I recognize that these types of studies are only the foundations to a much larger framework of

information that is still to come. Thus, one should learn from previous mistakes in order to progress in the long-term.

The method implemented here provides a greater resolution for studying the symmetry of a specific type of stone tool. The quantification of symmetrical measures combined with statistical analyses was useful for identifying trends within this study. It was shown using this methodology that tools should be scrutinized in much finer detail and that by looking at symmetry at the most minute levels can tell us a lot about how and why a tool would have been made in a particular way can be discovered. Although it is difficult to assume what early man was thinking when making these tools, it seems that the differences in symmetry of Acheulean tools for the sites Rietputs 15 and the Cave of Hearths could have been functionally driven.

Perhaps the most limiting factor to this study was its sample size and the inability to apply the methodology to tipless tools (thus leading to their exclusion). This should be something for future researchers to keep in mind when applying or adapting the method proposed here.

.

APPENDICES: CV TABLES SHOWING ALL DATA PRESENTED IN THIS STUDY

APPENDIX A: All data, Rietputs 15 Area

Tool ID	Site	Area/Volume	Max Width (cm)	Max Length (cm)	Max Thickness (cm)	Blank Type	Raw Material	Left Whole	Right Whole	Total Tool value	DS 1a (%)	DS 2a (%)	MS 1a (%)	Ms 2a (%)	PBS 1a (%)	PBS 2a (%)	Percent whole	Complete Distal (%)	Complete Medial (%)	Complete Proximal (%)	Absolute DS1a (mm²)	Absolute DS2a (mm²)	Absolute MS1a (mm²)	Absolute MS2a (mm²)	Absolute PBS1a (mm²)	Absolute PBS2a (mm²)	Absolute Distal (mm²)	Absolute Medial (mm²)	Absolute Proximal (mm²)
R99	Rietputs	Area	63.8	135.6	38.7	Flake	Hornfels	19313	22439	41752	11	11.3	20.3	22.5	15	19.9	100	27.1	40.7	32.2	24719.7	3480.7	3215.9	5031.9	5032.9	3862.6	28200.4	8247.83	8895.43
R102	Rietputs	Area	48.3	115.7	39.1	Indet	Chert	16343.1	17571.3	33914.4	10.2	11.4	20.4	22.8	17.6	17.7	100	23.5	42.2	34.2	37864	3173.7	5738.6	7829.6	8155.2	5694.1	41037.73	13568.15	13849.37
R107	Rietputs	Area	57.7	104.6	48.6	Cobble	Hornfels	16806.8	16206.7	33013.5	8.6	10.8	18	16.1	24.2	22.1	100	20.7	39.3	40	32856.5	2381.3	4416.9	6392.2	6529.3	6806.7	35237.75	10809.18	13336.01
R108	Rietputs	Area	77.5	144.4	53.2	Indet	Hornfels	25927.4	25381.5	51308.9	10.8	12.8	23.4	21.4	16.3	15.3	100	24.2	42.3	33.5	32412.2	3767.5	4065.2	7020.5	6693.2	5623.6	36179.71	11085.68	12316.81
R110	Rietputs	Area	45.9	27.8	35.1	Cobble	Hornfels	10583.5	9569.5	20153	13.9	6	20.4	18.9	18.2	22.6	100	21.5	43.2	35.3	3451.5	3851.6	6924.1	7722.4	5967.5	5997.3	7303.09	14646.5	11964.83
R172	Rietputs	Area	80.1	165.5	64.9	Flake	Qzite	30784.7	33069.5	63854.2	11	17.3	20.5	21.6	16.7	12.9	100	19.5	34.2	46.4	2847.6	3575.6	5957.6	5328.8	8001.5	7302.2	6423.21	11286.46	15303.75
R251	Rietputs	Area	61.9	110.6	60.4	Chunk	Qzite	20191.8	18195.9	38387.7	15	11.4	19.8	18	17.8	18	100	23.6	44.8	31.6	5563.4	6546.3	11993.5	10990.9	8370.6	7844.3	12109.69	22984.4	16214.82
R262	Rietputs	Area	51.8	98.6	36.2	Flake	Hornfels	11097.3	11544.9	22642.2	6.7	10.5	20.3	22.2	22	18.3	100	19.9	39.3	40.8	2808.6	1200.1	4103	3809.7	3671.8	4559.6	4008.72	7912.78	8231.43
R302	Rietputs	Area	63.4	102.1	50.5	Cobble	Chert	15064.9	16561.1	31626	9.6	11.9	18.5	21.1	19.6	19.3	100	28.2	42.1	29.7	7002	11030.6	13089.1	13798.1	10693.6	8240.8	18032.62	26887.2	18934.41
R328	Rietputs	Area	78.4	161	57.1	Cobble	Hornfels	28218.8	31343.2	59562	12.3	13.4	20.8	21.3	14.3	17.9	100	26.5	37.8	35.8	5762.8	4394.1	7611.5	6895.2	6817.5	6906.5	10156.91	14506.74	13724.08
R375	Rietputs	Area	66.6	126.3	48	Flake	V-lava	21556.5	19700.5	41257	15.1	9.2	19.6	20.2	17.5	18.3	100	17.2	42.5	40.3	1518.8	2382.5	4590.3	5024.8	4988.3	4137.6	3901.22	9615.13	9125.89
R378	Rietputs	Area	64.4	156.1	44.9	Flake	V-lava	18912.2	24236.5	43148.7	5.2	15.9	20	22	18.7	18.3	100	21.5	39.6	38.9	3035.2	3779.2	5837.7	6684.4	6192	6097.6	6814.37	12522.03	12289.57
R412	Rietputs	Area	56.1	132.1	45.1	Flake	V-lava	17821.1	18382.3	36203.4	16.3	9.2	20.4	22.2	12.6	19.3	100	25.7	42.1	32.2	7303.8	8004.7	12385.3	12667.4	8529.7	10671.1	15308.47	25052.7	19200.82
R466	Rietputs	Area	50	113.9	54.8	Flake Th	V-lava	15517.7	19837.1	35354.8	9.2	14.7	16.9	20.8	17.8	20.6	100	24.3	39.9	35.9	6215.3	3792.7	8102.4	8350.5	7238.9	7557.3	10007.94	16452.85	14796.23
R469	Rietputs	Area	51.2	100.2	27.9	Flake	Hornfels	10876.7	12222.1	23098.8	9.8	12.8	18.7	18.7	18.7	21.4	100	21.1	42	36.9	2225.9	6873.6	8636.7	9482.9	8049.6	7880	9099.5	18119.57	15929.61
R506	Rietputs	Area	56.4	126.1	53.8	Cobble-S	Hornfels	19630.8	18985.3	38616.1	8.1	16.1	20.4	19.4	22.4	13.6	100	25.5	42.6	31.9	5883.5	3342.7	7376.5	8043.9	4561.2	6995.7	9226.14	15420.32	11556.96
R539	Rietputs	Area	62.1	123.6	42.5	Flake	V-lava	19741.1	19329.7	39070.8	13.5	12.1	19.3	19.9	17.7	17.5	100	23.9	37.8	38.3	3251.4	5200.3	5987	7362.9	6279.3	7274	8451.62	13349.83	13553.38
R559	Rietputs	Area	52.2	107.4	43.5	Indet	Hornfels	13928.7	14559.4	28488.1	12.6	12.7	18.5	20.6	17.8	17.9	100	22.5	37.4	40	2252.9	2953.8	4315.6	4330.7	4308.1	4937.6	5206.72	8646.31	9245.8
R566	Rietputs	Area	49.6	100.3	38.5	Flake Co	Hornfels	14429.9	12649.9	27079.8	15.1	10	20.6	18.8	17.6	17.9	100	24.2	39.8	36	3113.8	6228	7866.2	7507.3	8650.9	5250	9341.83	15373.44	13900.86

R672	Rietputs	Area	60.5	117.9	47.9	Indet	Hornfels	1700 8.9	18277 .6	35286 .5	10.5	10.9	19.8	19.5	18	21.4	100	25.6	39.2	35.3	5271.6	4713.3	7536.6	7764.3	6932.9	6852.1	9984.84	15300 .94	13784.99
R746	Rietputs	Area	50.8	87.4	43.8	Flake	Hornfels	9717.2	11149	20866 .2	4.9	13.9	19.2	19.4	22.4	20.1	100	25.2	39.1	35.7	3586.3	3604.2	5283.1	5858	5059.4	5097.1	7190.48	11141 .11	10156.51
R770	Rietputs	Area	55.4	114.8	37.4	Flake	V-lava	1400 5.4	14610 .6	28616	8.8	11.7	21.7	19.4	18.5	19.9	100	25.1	39.3	35.6	4091.6	2704.1	5566.5	5085.5	4771.9	4860.3	6795.71	10651 .95	9632.18
R772	Rietputs	Area	77.6	168.6	34.6	Flake	V-lava	2889 8.5	32769 .9	61668 .4	6.6	19.8	19.8	22.5	20.5	10.8	100	21.4	39.2	39.3	3701.9	3851.5	6969.3	6880.3	6337.8	7545.8	7553.34	13849 .64	13883.6
R773	Rietputs	Area	52.4	122.8	57	Flake	V-lava	1694 4.7	17199 .6	34144 .3	13.9	14.8	19.3	21.7	16.4	13.9	100	18.8	38.6	42.5	1029.7	2896.2	4007.1	4055.7	4680.4	4197.2	3925.83	8062. 79	8877.63
R774	Rietputs	Area	62.1	139.6	42.8	Flake	Hornfels	1977 7.4	21222 .2	40999 .6	10.6	11.3	19.9	20.1	17.8	20.3	100	20.5	41.1	38.4	2507.6	3350.3	6203.9	5563.7	5293.9	5696.6	5857.92	11767 .58	10990.49
R788	Rietputs	Area	65.2	118.9	41.2	Flake Co	Hornfels	2010 1.1	18335	38436 .1	10.5	10.3	19.3	19.1	22.5	18.3	100	26.3	42.3	31.3	4046.8	12198 .2	12213	13883 .1	12638 .7	6688.7	16244 .96	26096 .1	19327.43
R793	Rietputs	Area	70.9	150.2	48.6	Flake	V-lava	2737 6.2	29769 .5	57145 .7	9.1	15.4	20.8	20.2	18	16.5	100	28.7	41	30.3	4753.7	5061.2	6587.8	7401.8	5603.2	4736.6	9814.86	13989 .66	10339.75
R804	Rietputs	Area	83.6	202.2	71.7	Flake	V-lava	4273 8.3	38467 .1	81205 .4	14.9	9.4	19	17.5	18.7	20.5	100	21.9	40	38.1	4339	4643.6	8153.4	8256.9	7285	8321.7	8982.56	16410 .35	15606.68
R852	Rietputs	Area	61.8	133	53.2	Flake	V-lava	2129 0.5	23005 .2	44295 .7	11.6	15.2	18.3	21.2	18.2	15.6	100	20.8	38.3	40.9	4040	3943.5	7399	7339.9	8662.1	7051.6	7983.48	14738 .89	15713.66
R961	Rietputs	Area	52.1	96.9	53.8	Flake	V-lava	1309 2.9	12448 .4	25541 .3	12.8	9.1	18.5	22.2	20	17.5	100	24.5	41	34.5	5205.4	8800.5	11912 .5	11536 .3	10258 .3	9432.7	14005 .88	23448 .8	19690.96
R1029	Rietputs	Area	47.7	109.2	44.7	Flake	V-lava	1237 5.2	12344 .5	24719 .7	14.1	13	20.4	20.4	15.6	16.6	100	24.4	36.5	39.1	12133 .3	7671.9	15450 .3	14171 .9	15154 .7	16623 .3	19805 .2	29622 .2	31778
R1031	Rietputs	Area	66.5	121.2	31.4	Indet	Hornfels	1669 7.5	21166 .5	37864	8.4	15.2	20.7	21.5	15	19.2	100	26.7	39.5	33.8	5131.5	6711.7	8112.4	9374.9	8046.6	6918.5	11843 .18	17487 .31	14965.19
R1052	Rietputs	Area	56.4	112.5	48.3	Indet	Hornfels	1558 0.2	17276 .3	32856 .5	7.2	13.4	19.5	19.9	20.7	19.3	100	21.8	40.7	37.5	3263.5	2315	4725.6	5668.5	5103.8	4464.8	5578.49	10394 .16	9568.63
R1060	Rietputs	Area	53.2	121.6	43.4	Flake	V-lava	1641 1.6	16000 .6	32412 .2	11.6	12.5	21.7	20.7	17.4	16.2	100	22.3	42.8	34.9	4572.9	4733.2	8471.2	9395.3	6268.9	8310.5	9306.11	17866 .46	14579.41
Mean			**60.4**	**122.6**	**46.54**			**1878 7.1**	**19583 .15**	**38370 .26**	**10.86**	**12.51**	**19.84**	**20.4**	**18.3**	**18.08**		**23.37**	**40.24**	**36.38**	**7581.28**	**4798.74**	**7376.61**	**7838.53**	**7083.19**	**6777.53**	**12380 .01**	**15215 .14**	**13860.74**
Std.Deviation			**10.17**	**29.57**	**9.5**			**6801.44**	**6923.52**	**13565 .41**	**2.98**	**2.75**	**1.26**	**1.56**	**2.5**	**2.65**		**2.76**	**2.17**	**3.77**	**9398.5**	**2467.96**	**2991.16**	**2807.35**	**2430.97**	**2359.96**	**9390.48**	**5722.45**	**4505.42**
Co-efficient of variation			**0.16**	**0.24**	**0.2**			**0.36**	**0.35**	**0.35**	**0.27**	**0.21**	**0.06**	**0.07**	**0.13**	**0.14**		**0.11**	**0.05**	**0.1**	**0.8**	**0.51**	**0.4**	**0.35**	**0.34**	**0.34**	**0.75**	**0.37**	**0.32**

APPENDIX B: All data, Cave of Hearths area

Tool ID	Site	Area/ Volume	Max Width (cm)	Max Length (cm)	Max Thickness (cm)	Blank Type	Raw Material	Left Whole	Right Whole	Total Tool value	DS1a (%)	DS2a (%)	MS1a (%)	Ms2a (%)	PBS1a (%)	PBS2a (%)	Percent whole	Complete Distal (%)	Complete Medial (%)	Complete Proximal (%)	Absolute DS1a (mm²)	Absolute DS2a (mm²)	Absolute MS1a (mm²)	Absolute MS2a (mm²)	Absolute PBS1a (mm²)	Absolute PBS2a (mm²)	Absolute Distal (mm²)	Absolute Medial (mm²)	Absolute Proximal (mm²)
coh11	CohC	Area	52.7	147	40.6	Flake Es	Quartz	17605.7	19426.8	37032.5	8.7	13	20.3	20.9	18.5	18.6	100	21.8	41.1	37.1	323 8.1	482 3.5	750 3.5	772 8.6	686 4.1	687 4.7	806 1.57	152 32.1 2	1373 8.82
coh203	CohC	Area	53.1	131.3	37.2	Flake Ss	Quartz	14401.1	16653.8	31054.9	6.2	13.2	20.1	21.9	20	18.5	100	19.4	42	38.5	193 1	410 7.7	625 5.1	680 0.1	621 5	574 6	603 8.68	130 55.2 2	1196 1.02
coh206	CohC	Area	41.3	36.2	67.7	Flake Cs	Qzite	16747.3	15150.4	31897.7	12.1	8.9	20.1	19.2	20.3	19.4	100	20.9	39.3	39.8	384 4.7	282 9.6	641 2.5	612 3	649 0	619 7.8	667 4.32	125 35.4 5	1268 7.86
coh287	CohC	Area	56.8	136.4	50.4	Flake	Qzite	20660.7	22341.7	43002.4	12.6	15.3	21.1	19.7	14.4	16.9	100	27.9	40.8	31.3	541 6.8	657 9.9	906 8.8	848 0.2	617 5	728 1.5	119 96.73	175 49.07	1345 6.53
coh304	CohC	Area	68.9	154.1	59.9	Indet Es	Qzite	27617.7	28919.1	56536.8	12	14.2	18.7	20	18.1	17	100	26.2	38.7	35.1	679 6.1	802 5.7	105 95.4	112 81	102 26.1	961 2.4	148 21.81	218 76.4	1983 8.49
coh340	CohC	Area	57.4	110.6	42.2	Flake Es	Qzite	17308.6	15727.9	33036.5	11.6	14.2	19.7	18.7	21.1	14.7	100	25.8	38.4	35.8	382 7.6	469 1.5	651 9.4	616 8	696 1.6	486 8.4	851 9.06	126 87.36	1183 0.05
coh365	CohC	Area	52	137.8	39.1	Flake	Qzite	18689.5	20791.7	39481.2	9.3	16.4	19.2	19.4	18.8	16.9	100	25.7	38.5	35.8	368 3.8	646 6.9	756 9.2	764 5.6	743 6.6	667 9.2	101 50.65	152 14.76	1411 5.83
coh419	CohC	Area	71.6	149.6	49	Indet	Dolerite	25060.4	28467.5	53527.9	10.1	16	19.9	21.1	16.8	16.1	100	26.1	41	32.9	538 2.2	857 5.6	106 72.4	112 88.8	900 5.8	860 3.2	139 57.81	219 61.2	1760 8.91
coh423	CohC	Area	75.4	144.6	53.6	Flake	Qzite	30748.8	29927.7	60676.5	14.6	14.3	20.1	18.7	16	16.3	100	28.9	38.8	32.3	886 5.5	865 1.7	121 90.7	113 70	969 2.6	990 6	175 17.22	235 60.72	1959 8.52
coh440	CohC	Area	68.8	119.5	36.9	Flake	Qzite	18574.4	19700.3	38274.7	8.9	11.3	19.6	19.4	20	20.7	100	20.2	39.1	40.7	340 5.5	433 4.7	752 0	743 4.9	764 8.9	793 0.8	774 0.22	149 54.82	1557 9.68
coh441	CohC	Area	58	116.7	32.2	Indet	Shale	16191.1	17370.3	33561.4	7.8	12.1	19.6	20.8	20.8	18.9	100	19.9	40.4	39.8	261 9.5	405 0.8	658 3.8	696 6.5	698 7.9	635 3	667 0.27	135 50.23	1334 0.93
coh444	CohC	Area	50.2	124.2	46.9	Indet	Dolerite	15925	17363.7	33288.7	11	13.4	20.4	19.5	16.5	19.2	100	24.4	39.9	35.7	365 1.1	446 7.5	678 1.9	650 3.1	549 2	639 3.1	811 8.64	132 85.04	1188 5.03
coh445	CohC	Area	60.5	139.8	44.5	Split Co	Chert	21302.8	22307.7	43610.5	11.8	11.1	18.3	18.9	18.7	21.1	100	22.9	37.2	39.8	516 1.1	483 1.2	797 9.6	826 3.3	816 2.1	921 3.3	999 2.32	162 42.84	1737 5.37
coh447	CohC	Area	50.2	118.2	38.1	Indet	Qzite	15715.1	14901.8	30616.9	13.4	10.2	21	19.7	16.9	18.7	100	23.6	40.7	35.6	411 3.7	312 2	642 5.4	604 5	517 5.9	573 4.7	723 5.77	124 70.45	1091 0.6
coh450	CohC	Area	65.8	80.4	45.4	Slab	Quartz	13845.1	14325.3	28170.4	7.1	9.4	16.8	18.9	25.2	22.6	100	16.6	35.6	47.8	201 2.9	265 1.9	472 9	531 2.5	710 3.3	636 0.9	466 4.73	100 41.51	1346 4.21
coh453	Coh	Area	63.5	134.6	55.6	Indet	Qzite	16455.1	23588	40043.1	8.7	14.2	21.9	23.9	10.5	20.8	100	22.9	45.8	31.3	349 0.4	569 1.9	876 0.9	956 6.2	420 3.8	832 9.8	918 2.29	183 27.17	1253 3.63

coh454	Coh Es	Area	47	103.8	32.2	Flake	Dolerite	10280.8	14405.5	24686.3	1.8	17.8	17.4	20.6	22.5	19.9	100	19.6	38	42.4	452.3	438	428	509	554	491	484	938	1046		
coh455	Coh Es	Area	65.3	155.5	56.8	Flake	Rhyolite	25645.6	27461.3	53106.9	8.7	11.9	20.1	20.9	19.4	18.9	100	20.6	41	38.4	462.1	633	106	110	103	100	55.02	217	2037		
coh458	Coh Es	Area	57.5	118.2	33.6	Flake	Dolerite	15472.1	17606	33078.1	3.5	14.4	21.1	19.8	22.2	19	100	17.9	40.9	41.2	115	477	696	654	735	628	592	135	1364		
coh460	Coh Es	Area	65.6	135	46.2	Flake	Dolerite	22704.5	21889.2	44593.7	12	14.9	21.6	19.6	17.3	14.6	100	26.9	41.2	31.9	535.2	665	963	872	771	651	120	59.09	1422		
coh462	Coh Es	Area	66	125.8	43.9	Slab	Dolerite Hornfels	19082.2	23901.9	42984.1	9.5	18.3	20.5	20.5	14.4	16.8	100	27.8	41	31.2	408	786	881	879	618	724	46.75	11.02	1342		
coh463	Coh Es	Area	62.1	130.9	55.3	Flake	Qzite	20887.4	20731.1	41618.5	10.7	13	19.1	21.5	20.4	15.3	100	23.6	40.7	35.7	443.3	539	796	896	849	637	982	23.99	1486		
coh480	Coh Es	Area	37.2	91.3	35.3	Flake	Qzite	7706.7	10780.9	18487.6	4.8	17.6	19.6	21.6	17.3	19	100	22.4	41.2	36.3	886.9	326	361	399	320	351	414	761	6719		
coh8022	Coh Es	Area	53.2	122.8	35.7	Flake	Quartz	15182.7	15816.6	30999.3	8.7	13.9	19.6	20.9	20.6	16.2	100	22.6	40.6	36.8	269	430	609	648	640	501	700	125 79.24	1141		
coh8069	Coh Es	Area	64.9	174.5	50.4	Indet	Qzite	22695.9	29608.9	52304.8	3.4	14.4	20.1	22.9	20	19.4	100	17.7	42.9	39.3	175	751	104	119	104	101	927	224	2057		
coh8089	Coh Es	Area	109.2	184.4	66.2	Flake	Qzite	53586.1	50014.7	10360.8	12.3	10.5	18.3	19.4	21.1	18.4	100	22.8	37.7	39.5	127 91.8	108 57.4	189 30.8	200 77.9	218 63.6	190 79.4	236 49.2	390 08.7	4094 3		
coh9001	Coh Es	Area	68.8	154.3	54.2	Flake	Chert	26400.1	25915.7	52315.8	10.4	10.1	19.5	20.1	20.5	19.3	100	20.5	39.6	39.9	542 6.1	530 0.9	102 27.7	104 99.5	107 46.3	101 15.3	26.96	207 27.2	2086 1.6		
coh e22	Coh Ind fl Cs	Area	49.9	125.1	33.6	Indet	Hornfels	14077.3	16462.4	30539.7	6	14.2	18.7	20.8	21.4	18.9	100	20.2	39.5	40.3	182 2.8	434 4.4	571 7.9	635 8.2	653 6.6	575 9.8	616 7.13	120 76.16	1229 6.37		
coh kj13	Coh Es	Area	42.7	87.2	34.3	Flake	Qzite	9130.2	10504.7	19634.9	8.4	15.2	19.9	20.5	18.2	17.8	100	23.7	40.4	35.9	165 8.5	298 8.8	390 5.2	402 8.1	356 6.5	348 7.9	464 7.24	793 3.32	7054 .38		
coh n17-coh pr24	Coh Es	Area	57.8	169.1	48.5	Flake	Quartz	22067.5	21701.2	43768.7	10.2	8.6	20.2	20	20	21	100	18.8	40.3	40.9	447 4.4	376 7.5	885 8.8	876 1	873 4.4	917 2.6	824 1.87	176 19.76	1790 7.04		
coh461	Coh Es	Area	64.4	124.6	31.3	Flake	Qzite	19078.1	18921.4	37999.5	12.4	11.4	19.7	19.7	18	18.7	100	23.8	39.4	36.8	472 0.3	432 1.8	750 0.9	747 5.4	685 7	712 4.3	904 2.04	149 76.21	1398 1.31		
	Coh Es	Area	58	116.6	46.8	Indet	Hornfels	17631.1	18410.6	36041.7	11.7	13.5	19.9	18.9	17.3	18.7	100	25.3	38.7	36	423 0.7	488 1.2	715 7.4	679 5.6	624 3	673 3.9	911 1.89	139 53	1297 6.91		
Mean			**59.86**	**128.12**	**45.11**			**19639.8968**	**20971.7437**	**40611.6406**	**9.387**	**13.406**	**19.731**	**20.262**	**18.85**	**18.438**		**22.73**	**40.01**	**37.24**	**399.75**	**533.5**	**801.48**	**820.09**	**762.65**	**742.15**	**933.25**	**162 20.57**	**1505 1.81**		
Std.Deviation			**12.81**	**28.88**	**10.01**			**8084.37**	**7451.63**	**15378.7**	**3.09**	**2.53**	**1.09**	**1.2**	**2.79**	**1.89**		**3.2**	**1.82**	**3.7**	**239 8.1**	**194 3.09**	**290 1.19**	**304 0.04**	**321 3.02**	**280 7.28**	**403 7.67**	**591 5.89**	**5909 .45**		
Co-efficient of variation			**0.21**	**0.22**	**0.22**			**0.41**	**0.35**	**0.37**	**0.32**	**0.18**	**0.05**	**0.05**	**0.14**	**0.1**		**0.14**	**0.04**	**0.09**	**0.59**	**0.36**	**0.36**	**0.37**	**0.42**	**0.37**	**0.43**	**0.36**	**0.39**		

APPENDIX C: All data, Rietputs 15 Volume

Tool ID	Site	Area/Volume	Max Width (cm)	Max Length (cm)	Max Thickness (cm)	Blank Type	Raw Material	Left Whole	*Right Whole*	Total tool value	DS 1a	DS 2a	MS1a	MS2a	PBS1a	PBS2a	Total (%)	Complete Distal (%)	Complete Medial (%)	Complete Proximal (%)	Absolute DS1a	Absolute DS2a	Absolute MS1a	Absolute MS2a	Absolute PBS1a	Absolute PBS2a	Absolute Distal	Absolute Medial	Absolute Proximal
R9901	Rietputs	Volume	63.8	135.6	38.7	Flake	Hornfels	7758.7	*9496.5*	1725.53	10.5	9.8	17.9	20.3	16.5	25	100	20.3	38.2	41.5	1812.1	1690.4	3095.3	3494.4	2851.3	4312.7	3502.5	6589.7	7163.1
R1022	Rietputs	Volume	48.3	115.7	39.1	Indet	Chert	5758.4	*7478.1.9*	1323.64	7.7	11.3	14.6	21.4	21.2	23.8	100	19	36	45	1013.9	1501.6	1936.7	2831.9	2808.8	3144.4	2514.5	4768.6	5953.2
R1077	Rietputs	Volume	57.7	104.6	48.6	Cobble	Hornfels	6909.2	*6645.1.7*	1355.41	4.7	7	11.7	9.3	34.6	32.7	100	11.8	21	67.3	6398.1	9536.5	1579.2	1261.5	4689.8	4430.6	1593.69	2840.7	9119.4
R1088	Rietputs	Volume	77.5	144.4	53.2	Indet	Hornfels	1168.56	*1292.33*	2460.89	13.4	17.5	20.6	22	13.5	13	100	30.9	42.6	26.5	3293.1	4303.4	5067.2	5417.9	3324.6	3202.9	7597.5	1048.1	6526.5
R1100	Rietputs	Volume	45.9	27.8	35.1	Cobble	Hornfels	3574.5	*3041.9.8*	6616.4.8	10.7	3.4	18.3	12.3	25	30.3	100	14.2	30.5	55.3	7110.7	2265.5	1207.5	8122.5	1655.5	2003.7	9375.65	2020.1.96	3658.7.2
R1721	Rietputs	Volume	80.1	165.5	64.9	Flake	Qzite	1069.90	*2089.20*	3159.10	5.6	18.1	9.8	24.8	18.5	23.2	100	23.7	34.6	41.7	1765.3	5727.3	3102.6	7826.0.8	5831.1.1	7338.5.8	7492.6.9	1092.86.4	1316.96.9
R2511	Rietputs	Volume	61.9	110.6	60.4	Chunk	Qzite	9399.6.5	*7697.4.4*	1709.70.9	15.7	10.9	17.4	14	21.9	20.1	100	26.6	31.4	42	2677.7.3	1865.9	2975.2	2395.9.5	3746.7.3	3435.5.9	4543.6.3	5371.1.5	7182.3.2
R2622	Rietputs	Volume	51.8	98.6	36.2	Flake	Hornfels	3937.6.4	*3593.9.7*	7531.6.1	2.6	3.8	9.8	12.3	39.9	31.7	100	6.4	22.1	71.6	1968.8	2827.8	7372.3	9237.9	3003.5.3	2387.4	4796.57	1661.0.17	5390.9.3
R3022	Rietputs	Volume	63.4	102.1	50.5	Cobble	Chert	5319.9.9	*7812.1.1*	1313.21	4.9	7.3	9.4	20.6	26.2	31.7	100	12.2	30	57.8	6478.3	9552.4	1235.3.8	2700.2.6	3436.7.8	4156.6.1	1603.0.73	3935.6.4	7593.3.9
R3288	Rietputs	Volume	78.4	161	57.1	Cobble	Hornfels	1200.28	*2017.44*	3217.72	7.9	14	14	20.8	15.5	28	100	21.8	34.8	43.4	2531.5	4490.8	4495.7.7	6689.1.4	4975.5.5	8994.4.2	7022.3	1118.49.1	1396.99.7
R3755	Rietputs	Volume	66.6	126.3	48	Flake	V-lava	7397.1.4	*9974.4.9*	1737.16.3	7.2	7.1	12.2	20.6	23.2	29.7	100	14.3	32.8	52.9	1243.0.9	1241.1.5	2123.3.7	3575.5.9	4030.6.8	5157.7.5	2484.2.4	5698.9.6	9188.4.3
R3788	Rietputs	Volume	64.4	156.1	44.9	Flake	V-lava	7737.8.3	*9528.4.9*	1726.63.2	4.8	15.6	17.6	17.9	22.5	21.7	100	20.4	35.4	44.1	8285.4	2698.7.5	3030.5.1	3085.4.9	3878.7.8	3744.2.4	3527.2.94	6116.0	7623.0.2
R4122	Rietputs	Volume	56.1	132.1	45.1	Flake	V-lava	6592.0	*7274.6.5*	1386.66.5	18	11.6	17.4	21.2	12.2	19.7	100	29.6	38.5	31.9	2493.7.8	1609.5.2	2410.7.9	2932.8.1	1687.4.3	2732.3.2	4103.3	5343.6	4419.7.5
R4666	Rietputs	Volume	50	113.9	54.8	Flake Th	V-lava	5925.3	*1028.85*	1621.38	5.8	13.3	10.6	18.9	20.1	31.2	100	19.1	29.6	51.3	9458.3	2158.3	1722.9.2	3072.0.8	3256.5.5	5058.0.9	3104.1.29	4795.0	8314.6.4
R4699	Rietputs	Volume	51.2	100.2	27.9	Flake	Hornfels	2202.0.1	*4100.6.5*	6302.6.6	4.3	13.6	8.2	18.1	22.4	33.4	100	17.9	26.3	55.8	2709.1	8578.8	5190.9	1140.5.5	1412.0.2	2102.2.2	1128.7.89	1659.6.36	3514.2.4
R5066	Rietputs	Volume	56.4	126.1	53.8	Cobble-S	Hornfels	6893.7.2	*1031.40*	1720.77.2	4.4	15.6	10.9	23.1	24.8	21.3	100	20	33.9	46.1	7492.6	2688.4.7	1873.7.5	3967.7	4270.7.1	3657.8	3437.7.27	5841.4.5	7928.5.1
R5389	Rietputs	Volume	62.1	123.6	42.5	Flake	V-lava	9493.8	*6566.8*	1606.06	13.7	7.9	21	11.9	24.4	21.1	100	21.6	32.9	45.5	2208.2.4	1267.2.4	3373.6	1904.7.8	3911.9.6	3394.7.8	3475.4.8	5278.3.8	7306.7.4
R5599	Rietputs	Volume	52.2	107.4	43.5	Indet	Hornfels	4400.6.6	*6109.4.9*	1051.01.5	11.3	13.9	11.5	21.5	19.1	22.8	100	25.2	33	41.8	1187.6.2	1460.6.4	1207.6.6	2256.6.4	2005.3.8	2392.2.1	2648.2.6	3464.3	4397.5.9

R566	Rietputs	Volume	49.6	100.3	38.5	Flake Co	Hornfels	3565 7.3	*6131 7.2*	9697 4.5	9	10.2	11.9	21.2	15.9	31.8	100	19.1	33.2	47.7	8701.5	9859.9	1158 0.8	2059 1.3	1537 5.1	3086 6	1856 1.34	3217 2.1	4624 1.1
R672	Rietputs	Volume	60.5	117.9	47.9	Indet	Hornfels	5882 5.9	*7485 1.9*	1336 77.8	7.3	11.1	14.8	17.2	21.9	27.8	100	18.4	31.9	49.7	9777.7	1477 3.6	1973 6.8	2293 3.5	2931 1.4	3714 4.7	2455 1.32	4267 0.3	6645 6.1
R746	Rietputs	Volume	50.8	87.4	43.8	Flake	Hornfels	2750 6.2	*3786 0.8*	6536 7	2.3	9.5	10.2	18.8	29.6	29.6	100	11.8	29	59.2	1485.7	6225 .2	6644 .2	1229 1.5	1937 6.3	1934 4.1	7710 .87	1893 5.68	3872 0.4
R770	Rietputs	Volume	55.4	114.8	37.4	Flake	V-lava	3872 3	*6094 5.6*	9966 8.6	4.6	10.4	12.5	17.9	21.8	32.8	100	15	30.4	54.6	4589.5	1040 2	1241 6.3	1784 5.1	2171 7.1	3269 8.6	1499 1.53	3026 1.4	5441 5.7
R772	Rietputs	Volume	77.6	168.6	34.6	Flake	V-lava	1574 93	*1794 23*	3369 16	5.2	19.4	15.7	21.3	25.8	12.5	100	24.6	37	38.4	1762 5	6535 9.4	5285 4.7	7182 3.2	8701 2.9	4224 0.6	8298 4.4	1246 77.9	1292 53.5
R773	Rietputs	Volume	52.4	122.8	57	Flake	V-lava	4454 7.2	*8038 1.6*	1249 28.8	15.8	23.6	10.1	23.1	9.7	17.7	100	39.4	33.2	27.4	1976 7.9	2947 7	1263 3.5	2882 8.3	1214 5.8	2207 6.3	4924 4.9	4146 1.8	3422 2.1
R774	Rietputs	Volume	62.1	139.6	42.8	Flake	Hornfels	6159 3.3	*1130 56*	1746 49.3	8	16.4	14.1	21.8	13.1	26.5	100	24.5	35.9	39.6	1402 5.4	2870 9.8	2461 6.5	3813 5.4	2295 1.5	4621 0.4	4273 5.2	6275 1.9	6916 1.9
R788	Rietputs	Volume	65.2	118.9	41.2	Flake Co	Hornfels	8228 2	*8205 5.3*	1643 37.3	9.6	11	14.8	16.5	25.7	22.4	100	20.6	31.2	48.1	1582 2.5	1809 1.3	2424 7.9	2710 4.9	4221 1.6	3685 9	3391 3.8	5135 2.8	7907 0.6
R793	Rietputs	Volume	70.9	150.2	48.6	Flake	V-lava	1068 60	*1972 78*	3041 38	3.6	14.5	12	22.1	19.5	28.3	100	18.2	34.1	47.8	1108 6.4	4411 7.7	3653 5.2	6710 3.5	5923 8.1	8605 6.5	5520 4.1	1036 38.7	1452 94.6
R804	Rietputs	Volume	83.6	202.2	71.7	Flake	V-lava	2024 96	*2652 68*	4677 64	11.8	11.6	11.6	16.4	19.8	28.6	100	23.5	28.1	48.5	5530 9.1	5445 1.5	5443 0.8	7691 6.9	9275 5.9	1338 99	1097 60.6	1313 47.7	2266 54.9
R852	Rietputs	Volume	61.8	133	53.2	Flake	V-lava	7758 6.1	*1397 17*	2173 03.1	8.4	18.1	9.8	24.4	17.5	21.8	100	26.5	34.3	39.3	1819 2.7	3931 4.9	2139 7.4	5309 1.2	3799 6	4731 0.8	5750 7.6	7448 8.6	8530 6.8
R961	Rietputs	Volume	52.1	96.9	53.8	Flake	V-lava	3965 2.9	*5976 9.8*	9942 2.7	10.8	10.1	10	26	19.1	24	100	20.9	36	43.1	1071 6.2	1004 3.3	9904 .7	2589 7.8	1903 2	2382 8.7	2075 9.5	3580 2.46	4286 0.7
R1029	Rietputs	Volume	47.7	109.2	44.7	Flake	V-lava	2587 8.2	*5449 1.6*	8036 9.8	7.4	14.1	7.4	24.1	17.4	29.6	100	21.6	31.5	47	5980	1134 7.2	5941 .1	1935 9.4	1395 7.1	2378 5.1	1732 7.22	2530 0.48	3774 2.2
R1031	Rietputs	Volume	66.5	121.2	31.4	Indet	Hornfels	9398 5.3	*7045 1*	1644 36.3	8.5	10.1	21	11.9	27.6	20.9	100	18.6	32.8	48.6	1402 2.5	1658 8	3449 9.5	1948 8.7	4546 3.3	3437 4.4	3061 0.5	5398 8.2	7983 7.7
R1052	Rietputs	Volume	56.4	112.5	48.3	Indet	Hornfels	5495 0.6	*7662 2*	1315 72.6	3.8	12.3	11.4	18.6	26.6	27.3	100	16.1	30	53.9	4978 .6	1623 4	1503 0.8	2443 6.7	3494 1.2	3595 1.2	2121 2.57	3946 7.5	7089 2.4
R1060	Rietputs	Volume	53.2	121.6	43.4	Flake	V-lava	5910 1.9	*7153 0.3*	1306 32.2	10	14.5	16.1	19.8	19.1	20.4	100	24.5	35.9	39.6	1305 5.2	1899 6.6	2104 2.7	2584 4.4	2500 4	2668 9.3	3205 1.8	4688 7.1	5169 3.3
Mean			**60.4**	**122.6**	**46.54**			**7188 2.81**	***9600 4.14***	**1678 86.95**	**8.21**	**12.31**	**13.42**	**19.17**	**21.51**	**25.36**		**20.53**	**32.59**	**46.88**	**1403 8.36**	**2217 0.15**	**2295 4.62**	**3278 1.42**	**3488 9.8**	**4105 2.5**	**3620 8.52**	**5573 6.04**	**7594 2.3**
Std.Deviation			**10.17**	**29.57**	**9.5**			**3825 8.8**	***5510 2.64***	**9013 2.44**	**3.97**	**4.34**	**3.74**	**4.13**	**6.16**	**5.53**		**6.25**	**4.3**	**9.58**	**1051 3.37**	**1615 3.27**	**1346 5.21**	**1967 1.82**	**1873 3.73**	**2348 2.6**	**2404 5.91**	**3127 8.87**	**3974 6.34**
Co-efficient of variation			**0.16**	**0.24**	**0.2**			**0.53**	***0.57***	**0.53**	**0.48**	**0.35**	**0.27**	**0.21**	**0.28**	**0.21**		**0.3**	**0.13**	**0.2**	**0.74**	**0.72**	**0.58**	**0.6**	**0.53**	**0.57**	**0.66**	**0.56**	**0.52**

APPENDIX D: All data, Cave of Hearths Volume

Tool ID	Site	Area/Volume	Max Width (cm)	Max Length (cm)	Max Thickness (cm)	Blank Type	Raw Material	Left Whole	Right Whole	Total tool value	DS 1a	DS 2a	MS1a	MS2a	PBS1a	PBS2a	Total (%)	Complete Distal (%)	Complete Medial (%)	Complete Proximal (%)	Absolute DS1a	Absolute DS2a	Absolute MS1a	Absolute MS2a	Absolute PBS1a	Absolute PBS2a	Absolute Distal	Absolute Medial	Absolute Proximal
coh11	CohC	Volume	52.7	147	40.6	Indetfl	Quartz	5535	8545	1408	5.4	13.4	12.5	20.9	21.5	26.4	100	18.8	33.4	47.8	7581	1892	1755	2942	3021	3710	2650	4697	6732
coh203	CohC	Volume	53.1	131.3	37.2	Flake	Quartz	2738	8009	1074	3.1	16.5	8.3	31.8	14.2	26.2	100	19.5	40.1	40.4	3279.9	1773	8879.1	3420	1522	2815	2101	4308	4338
coh206	CohC	Volume	41.3	36.2	67.7	Flake	Qzite	4785	6576	1136	8.6	9.9	11.5	18.8	22.1	29.2	100	18.5	30.2	51.2	9748.7	1130	1302	2132	2508	3314	2104	3434	5822
coh287	CohC	Volume	56.8	136.4	50.4	FlakeCs	Qzite	8961	1056	1952	17.2	20.3	18.9	19.1	9.8	14.7	100	37.5	37.9	24.5	3357.5	3970	3687	3721	1916	2875	7327	7409	4791
coh304	CohC	Volume	68.9	154.1	59.9	FlakeEs	Qzite	1305	1637	2942	10.4	13.8	13.3	19.5	20.6	22.4	100	24.2	32.8	43	3061.1	4069	3924	5724	6070	6579	7131	9648	1264
coh340	CohC	Volume	57.4	110.6	42.2	Flake	Qzite	7557	3157	1071	17.7	9.5	25.4	10.8	27.5	9.2	100	27.2	36.1	36.7	1896.4	1015	2717	1154	2943	9873	2912	3871	3930
coh365	CohC	Volume	52	137.8	39.1	Flake	Qzite	6371	8730	1510	8	20.3	15.1	19.1	19.1	18.4	100	28.3	34.2	37.5	1205.1	3064	2281	2886	2884	2778	4269	5168	5663
coh419	CohC	Volume	71.6	149.6	49	Indet	Dolerite	9587	1566	2524	6	14.9	12.1	22.9	20	24.2	100	20.8	35	44.2	1505.6	3755	3043	5786	5037	6120	5260	8830	1115
coh423	CohC	Volume	75.4	144.6	53.6	FlakeEs	Qzite	1856	1660	3516	14.7	12.1	18.5	14.7	19.6	20.4	100	26.8	33.3	39.9	5154.1	4271	6523	5172	6886	7158	9426	1169	1404
coh440	CohC	Volume	68.8	119.5	36.9	Flake	Qzite	5476	6693	1217	5.6	8.2	10.7	15.6	28.8	31.3	100	13.7	26.2	60	6786.3	9923.8	1297	1896	3500	3804	1671	3193	7305
coh441	CohC	Volume	58	116.7	32.2	Slab	Shale	5164	6768	1193	6.2	10.1	14.2	21.4	22.9	25.2	100	16.3	35.6	48.1	7434.7	1207	1693	2553	2726	3007	1950	4247	5734
coh444	CohC	Volume	50.2	124.2	46.9	IndetEs	Dolerite	5343	7742	1308	6.7	11.3	13.5	15.5	20.6	32.4	100	18	29	53	8767.5	1477	1770	2024	2696	4240	2354	3795	6937
coh445	CohC	Volume	60.5	139.8	44.5	FlakeEs	Chert	7158	1045	1761	11.5	14.3	12	19.8	17.1	25.2	100	25.9	31.8	42.3	2033	2527	2118	3487	3006	4441	4561	5605	7448
coh447	CohC	Volume	50.2	118.2	38.1	FlakeEs	Qzite	4327	7341	1166	8.1	11.5	12.1	21.2	16.9	30.3	100	19.6	33.3	47.2	9414.6	1341	1415	2468	1971	3531	2282	3884	5502
coh450	CohC	Volume	65.8	80.4	45.4	Flake	Quartz	5711	4948	1066	4.4	4.9	10.3	11.9	38.9	29.7	100	9.3	22.1	68.6	4681.5	5238.5	1092	1264	4150	3160	9919	2356	7311
coh453	CohC	Volume	63.5	134.6	55.6	Flake	Qzite	9368	8288	1765	14	14.3	28.1	16.8	11	15.8	100	28.3	44.8	26.8	2468.4	2533.2	4952	2961	1947	2793	5001	7914	4740
coh454	CohC	Volume	47	103.8	32.2	Indet	Dolerite	3278	4500	7779	0.7	14.1	11.1	16.2	30.3	27.6	100	14.7	27.3	57.9	527.2	1094	8655.1	1261	2360	2144	1147	2127	4504
coh455	CohC	Volume	65.3	155.5	56.8	Slab	Dolerite	1092	1503	2595	5	10.4	13.7	19.7	23.4	27.9	100	15.4	33.3	51.3	1301	2695	3546	5107	6074	7231	3997	8654	1330

coh458	Coh	Volume	57.5	118.2	33.6	Inset	Dolerite	57384	6717	1245	1.9	13.2	17	17.5	27.1	23.2	100	15.1	34.5	50.3	2426.4	1641	2118	2181	3377	2893	1884	4299	6271
coh460	Coh	Volume	65.6	135	46.2	Split Co	Igneous	79532	1059	1854	9	15.6	14.4	20.4	19.5	21.2	100	24.6	34.8	40.6	1668.1	2891	2672	3774	3612	3925	4560	6446	7538
coh462	Coh	Volume	66	125.8	43.9	Inset Es	Dolerite	79635.4	1142	1938	10.2	20.5	17.9	20.6	13	17.9	100	30.7	38.5	30.8	1979.2	3973	3470	3984	2513	3464	5953	7454	5978
coh463	Coh	Volume	62.1	130.9	55.3	Flake	Hornfels	59404.9	1164	1758	5.9	16.7	8.5	26.9	19.4	22.6	100	22.6	35.4	42	1033.7	2936	1490	4732	3416	3978	3970	6223	7394
coh480	Coh	Volume	37.2	91.3	35.3	Flake	Qzite	143293	1987	3420	5.9	7.4	21.9	24.9	14.1	25.9	100	13.3	46.8	40	2026.6	2517	7482	8508	4820	8849	4543	1599	1367
coh802	Coh	Volume	53.2	122.8	35.7	Flake	Quartz	53357.3	4883	1021	10.6	14.7	17.6	17.8	24.1	15.4	100	25.3	35.3	39.4	1083.5	1499	1794	1814	2457	1569	2583	3608	4027
coh806	Coh	Volume	64.9	174.5	50.4	Inset Es	Qzite	68220.9	1444	2126	0.9	11.6	9.2	25.4	21.9	31	100	12.5	34.6	52.9	1959.3	2461	1959	5400	4666	6583	2657	7359	1124
coh808	Coh	Volume	109.2	184.4	66.2	Flake Es	Qzite	29026	3591	6494	7.3	9.2	10.5	16.9	26.9	29.2	100	16.4	27.5	56.1	4708.6	5960	6842	1098	1747	1897	1066	1782	3644
coh900	Coh	Volume	68.8	154.3	54.2	Flake Es	Chert	11203	1135	2256	7.1	7.2	13.9	15	28.7	28.1	100	14.3	28.9	56.8	1603.7	1621	3134	3392	6464	6344	3225	6527	1280
cohe22	Coh	Volume	49.9	125.1	33.6	Flake	Hornfels	43093.7	6518	1082	6	16.5	13.3	22.3	20.5	21.4	100	22.4	35.7	41.9	6447.9	1781	1444	2417	2220	2318	2426	3862	4538
cohkj13	Coh	Volume	42.7	87.2	34.3	Inset Cs	Qzite	45632.4	1592	6156	7.4	0.5	25.6	1.2	41.2	24.2	100	7.9	26.8	65.3	4567	291.1	1573	741.9	2533	1489	4858	1647	4022
cohn17-pr24	Coh	Volume	57.8	169.1	48.5	Flake Ss	Quartz	43340.9	1210	1643	3.5	10.2	5.7	26.2	17.2	37.3	100	13.7	31.9	54.5	5765.3	1673	9296.7	4305	2827	6123	2249	5234	8950
coh461	Coh	Volume	58	116.6	46.8	Inset	Hornfels	39382	1115	1508	1.9	14.8	7.1	22.5	17.1	36.6	100	16.7	29.6	53.7	1033.7	2936	1490	4732	3416	3978	3970	6223	7394
Mean			**59.86**	**128.12**	**45.11**			**79115**	**1031**	**1822**	**7.54**	**12.35**	**14.43**	**18.59**	**21.98**	**24.81**		**19.88**	**33.32**	**46.78**	**1452.8**	**2259.1**	**2616.8**	**3558.6**	**3904.0**	**4513.2**	**3711.9**	**6175.1**	**8417.6**
Std.Deviation			**12.81**	**28.88**	**10.01**			**5163.15**	**6314.22**	**1110.37**	**4.28**	**4.46**	**5.34**	**5.62**	**7.07**	**6.27**		**6.64**	**5.11**	**10.19**	**1210.45**	**1291.16**	**1725.84**	**2202.58**	**2843.64**	**3240.23**	**2351.54**	**3642.79**	**5977.83**
Co-efficient of variation			**0.21**	**0.22**	**0.22**			**0.65**	**0.61**	**0.6**	**0.56**	**0.36**	**0.37**	**0.29**	**0.32**	**0.25**		**0.33**	**0.15**	**0.21**	**0.83**	**0.57**	**0.65**	**0.61**	**0.72**	**0.71**	**0.63**	**0.58**	**0.71**

REFERENCES

Archer, W. and Braun, D. R. 2010. Variability in bifacial technology at Elandsfontein, Western Cape, South Africa: a geometric morphometric approach. *Journal of Archaeological Science* 37: 201-209.

Asfaw, B. Beyene, Y. Suwa, G., Walter, R. C. White, T. D. Woldegabrieal, G. and Yemane, T. 1992. The earliest Acheulean from Konso Gardula. *Nature* 360: 732-735.

Beyene, P.Y. Suwa, G., Katoh, S. Asfaw, B. 2007. The beginning of the Acheulean culture in its environmental context at Konso, Ethiopia. Abstract. In: de Lumley, H. (ed.), *Les Cultures à Bifaces du Pléistocene Inferieur et Moyen dans le Monde. Émergence du Sens de l' Harmonie*. Nice: Edudud.

Brande, S. & Saragusti, I. 1996. A Morphometric Model and Landmark Analysis of Acheulean Handaxes from Northern Israel. In: Marcus, L. F. *et al* (eds), *Advances in Morphometrics.* Plenum Press, New York. pp. 225-243.

Cardillo, M. 2010. Some applications of Geometric Morphometrics to archaeology. In: Elewa, A. M. T. (eds), Morphometrics for Nonmorphotericians. *Lecture Notes in Earth Science 124*. Springer, Dordrecht, pp. 325-341.

Clark, J. D. 2001. Variability in primary and secondary technologies of the Later Acheulean in Africa. In: Milliken, S. & Cook, J. (eds) *A Very Remote Period Indeed:1-18* Oxford, Oxbow Books.

Clarkson, C. 2006. Quantifying flake scar patterning on cores using 3D recording techniques. *Journal of Archaeological Science* 33: 132-142.

Crompton, R. H. and Gowlett, J. A. J. 1993. Allometry and multidimensional form in Acheulean bifaces from Kilombe, Kenya. *Journal of Human Evolution* 25: 175-199.

Domínguez-Rodrigo, M. and de la Torre, I. 2002. The ST Site Complex at Peninj, West Lake Natron, Tanzania: Implications for Early Hominid Behavioural Models. *Journal of Archaeological Science 29*, 639-665.

Gibbon, R. J., Granger, D. E., Kuman, K. and Partridge, T. C. 2009. Early Acheulean technology in the Rietputs formation, South Africa, dated with cosmogenic nuclides. *Journal of Human Evolution* 56: 152-160.

Goren-Inbar, N. & Sharon, G. 1999. Soft percussor use at the Gesher Benot Ya'aqov Acheulean Site? *Journal of The Prehistoric Society* 28: 55-79.

Goren-Inbar, N. and Sharon, G. 2006. Invisible handaxes and visible Acheulean biface technology at Gesher Benot Ya'aqov, Israel. In: Goren-Inbar, N. and Sharon, G. (eds), *Axe Age: Acheulean Tool-making from Quarry to Discard:* 111-136. London, Equinox.

Gowlett, A., J. 2011. The Vital Sense of Proportion: Transformation, Golden Section, and 1:2 Preferences in Acheulean Bifaces. *Paleoanthropology*, 174-187.

Grosman, L., Goldsmith, Y., Smilansky, U. 2011. Morphological Analysis of Nahal Zihor Handaxes: A Chronological Perspective. *Paleoanthropology*. 203-215.

Grosman, L., Smikt, O. and Smilansky, U. 2008. On the application of 3-D scanning technology for the documentation and typology of lithic artifacts. *Journal of Archaeological Science* 35: 3101-3110.

Hardaker, T. & Dunn, S. 2005. The Flip Test – a new statistical measure for quantifying symmetry in stone tools. *Antiquity* 79 (306)> File:///C:/Documents%20 and%20settings/09400149/

My%20Documents/OLD%20C%20drive%20Files/flip%20test%20antiquity,%20Project%20Gallery%20Hardaker%20&%20Dunn.mht

Hay, R. L. 1976. *Geology of the Olduvai Gorge: A Study of Sedimentation in a Semi-Arid Basin.* Berkeley: University of California Press.

Isaac, G. L. 1997. *Koobi Fora Research Project, Vol 5, Plio-Pleistocene Archaeology.* Oxford: Clarendon Press.

Klein, R. 2000. The Earlier Stone Age of southern Africa. *South African Archaeological Bulletin* 55: 107-122.

Kuman, K., Gibbon, R. J. in press. The early Acheulean of South Africa: Sterkfontein valley and the Vaal River Basin. In: de Lumley, H (eds), *Les Cultures à Bifaces du Pleistocene Inferieur et Moyen dans le Monde*. Émergence du sens de l'Harmomie. Nice: Edusud.

Kuman, K. 2007. The Earlier Stone Age in South Africa: site context and the influence of cave studies. In: Pickering, T. R. Schick, K. and Toth, N. (eds), *Breathing Life into Fossils: Taphonomic Studies in Honour of C. K. (Bob) Brain*. Bloomington (Indiana): Stone Age Institute Press, pp 181-198.

Kuman, K., Field, A., S. & Thackery, J., F. 1997. Discovery of new artefacts at Kromdraai. *South African Journal of Science 93*: 187-193.

Kuman, K. & R.J. Clarke 2000. Stratigraphy, artefact industries and hominid associations for Sterkfontein, Member 5. *Journal of Human Evolution* 38: 827-847.

Leader, G. M. 2009. *Early Acheulean in the Vaal River basin, Rietputs Formation, Northern Cape Province, South Africa*. MSc Dissertation. University of the Witwatersrand.

Lepre, C. J., Roche, H., Kent, D. V., Harmand, S., Quinn, L. R., Brugal, J., Texier, P., Lenoble, A., Feibel, C. S., 2011. An earlier origin for the Acheulian. *Nature 477*. 82-85.

Lin, S. C. H., Douglass, M. J., Holdaway, S. J., Floyd, B. 2010. The application of 3D laser scanning technology to the assessment of ordinal and mechanical cortex quantification in lithic analysis. *Journal of Archaeological Science 37*: 694-702.

Lycett, S. J., von Cramon-Taubadel, N., Foley, R. 2006. A crossbeam co-ordinate calliper for morphometric analysis of lithic nuclei: a description, test and empirical examples of application. *Journal of Archeological Science 33*. 847-861.

Mason, R. J. 1962. *Prehistory of the Transvaal*. Johannesburg: Witwatersrand University Press.

Minium, E., W. 1978. Statistical Reasoning in Psychology and Education (2nd ed). New York, John Wiley & Sons.

McNabb, J. Binyon, F. Hazelwood, L. 2004. The Large Cutting Tools from the South African Acheulean and the Question of Social Traditions. *Current Anthropology* 45: 653-677.

McPherron, S. P. 2000. Handaxes as a measure of mental capabilities of early hominids. *Journal of Archaeological Science* 27: 655-663.

Pickering, T. R., Egeland, C. P., Domínguez-Rodrigo, M., Brain, C. K., Schnell, A. G. 2008. Testing the ‘’shift in the balance of power’’ hypothesis at Swartkrans, South Africa: Homonid cave use and subsistence behaviour in the Early Pleistocene. *Journal of Anthropological Archaeology 27*: 30-45.

Porat, N. Chazan, M. Grun, R. Aubert, M. Eisenmann, V. and Horwitz, K. L. 2010. New radiometric ages for the Fauresmith industry from Kathu Pan, southern Africa: implications for the earlier to Middle Stone Age transition. *Journal of Archaeological Science* 37*:* 269-283.

Posnansky, M. 1959. Some Functional Considerations on the Handaxes. *Man 61*. 42-44.

Potts, R. 1989. Olargesailie: new excavations and findings in Early and Middle Pleistocene contexts, southern Kenya rift valley. *Journal of Human Evolution 18:* 477-484.

Roe, D., A. 1964. The British Lower and Middle Paleolithic: some problems. Methods of study and preliminary results. *Preceedings of the Prehistoric Society 30*. 245-267.

Roe, D.,A. 1994. Summary and overview. In M.D. Leakey and D.A. Roe (eds): *Olduvai Gorge, Vol. 5*. Cambridge: Cambridge University Press.

Saragusti, I. Karasik, A. Sharon, I. and Smilansky, U. 2005. Quantitative analysis of shape attributes based on contours and section profiles in artifact analysis. *Journal of Archaeological Science* 32: 841-853.

Saragusti, I. Sharon, I. Katzenelson, O. and Avnir, D. 1998. Quantitative analysis of the symmetry of artefacts: Lower Paleolithic handaxes. *Journal of Archaeological Sciences* 25: 817-825.

Schick, K. and Toth, N. 1995. The importance of Actualistic Studies in Early Stone Age Research: Some Personal reflections. In Schick, K. and Toth, N. (eds), *The Cutting Edge: New Approaches to the Archaeology of Human Origins 3*, 267-344.

Sumner, T. A. and Riddle, T. R. A. 2008. A virtual Paleolithic: assays in photogrammetric Three Dimensional Artifact Modelling. *Paleoanthropology*: 158-169.

Tobias, P., V. 1971 Human skeletal remains from the Cave of Hearths, Makapansgat, Northern Transvaal. *American Journal of Physical Anthropology 34*: 335-367.

Toth, N. 1985. The Oldowan reassessed: a close look at early stone artifacts. *Journal of Archaeological Science* 12: 101-120.

Underhill, D. 2007. Subjectivity inherent in by-eye symmetry judgements and the large cutting tools at the Cave of Hearths, Limpopo Province, South Africa. *Papers from the Institute of Archaeology* 18: 1-12.

van Riet Lowe, C. 1945. The evolution of the Levallois Technique in South Africa. *Man* XLV: 37-51.

Wynn, T., Tierson, F., 1990. Regional comparison of the shapes of later Acheulean handaxes. *American Anthropologist 92*. 73-84.

Wynn, T. 1995. Handaxe Enigmas. *World Archaeology* 27: 299-322